# Discovery of Novel Biased Opioid Receptor Ligands through Structure-Based Pharmacophore Virtual Screening and Experiment

*Pyeonghwa Jeong[#,4], Soo-Kyung Kim[#,1], Quanjie Li[1,2,3], Su-jin Oh[5], Seonil Son[5], Guangju Chen[2], Hongwei Tan[2],* Siwon Kim[6,7], Jong-Hyun Park[6], Ki Duk Park[6,7,8], *Yeo Ok Kim[9], Myung Ha Yoon[9], Yong-Chul Kim[4,5*], William A. Goddard III[1*]*

[a] Prof. William A. Goddard III
[1]Materials and Process Simulation Center (MC-139-74), California Institute of Technology, Pasadena, California 91125, US
E-mail: wag@caltech.edu ORCID:0000-0003-0097-5716;
Prof. Y.-C. Kim
[5]School of Life Sciences, [4]Department of Biomedical Science & Engineering, Gwangju Institute of Science & Technology
123 Cheomdan-gwagiro, Buk-gu, 61005, South Korea
E-mail: yongchul@gist.ac.kr

[b] PH. Jeong
[4]Department of Biomedical Science & Engineering, Gwangju Institute of Science & Technology, 123 Cheomdan-gwagiro, Buk-gu, 61005, South Korea
Dr. S-K. Kim
[1]Materials and Process Simulation Center (MC-139-74), California Institute of Technology, Pasadena, California 91125, US
Dr. Q. Li
[1]Material and Process Simulation Center (MC-139-14)
[2]College of Chemistry, Beijing Normal University
Beijing, 100875, People's Republic of China
[3]Institue of Medicinal Biotechnology, Chinese Academy of Medical Science, Beijing, 100050, People's Republic of China
S. Oh, S. Son
[5]School of Life Sciences, Gwangju Institute of Science & Technology
123 Cheomdan-gwagiro, Buk-gu, 61005, South Korea
Prof. G. Chen, Prof. H. Tan
[2]College of Chemistry, Beijing Normal University
Beijing, 100875, People's Republic of China
S. Kim
[6]Convergence Research Center for Diagnosis, Treatment and Care system of Dementia, Korea Institute of Science and Technology (KIST), Seoul 02792, South Korea
[7]Division of Bio-Medical Science & Technology, KIST School, Korea University of Science and Technology, Seoul 02792, South Korea
Dr. J-H. Park
[6]Convergence Research Center for Diagnosis, Treatment and Care system of Dementia, Korea Institute of Science and Technology (KIST), Seoul 02792, South Korea
Dr. K.D. Park
[6]Convergence Research Center for Diagnosis, Treatment and Care system of Dementia, Korea Institute of Science and Technology (KIST), Seoul 02792, South Korea
[7]Division of Bio-Medical Science & Technology, KIST School, Korea University of Science and Technology, Seoul 02792, South Korea
[8]KHU-KIST Department of Converging Science and Technology, Kyung Hee University, Seoul 02447, South Korea
Prof. M.H. Yoon, Dr. Y.O. Kim
[9]Department of Anesthesiology and Pain Medicine, Medical School, Chonnam National University, Gwangju 501-757, South Korea

**Table S1.** Top10 predicted active ensembles structures of human mu opioid receptor (μ-OR) from the BiHelix procedure. Four different energies, charged total energy (CTotal), charged interhelical (CInterH), neutral total (NTotal) and neutral interhelical (NInterH) energy, associated with each 7-helix (H) bundles were evaluated and ranked. The structures were ordered by the average rank of these four energies (RankCNti). Chosen 3 conformers for SuperBiHelix sampling are all-zero structures modeled from active μ-OR, inactive δ-OR, and inactive  -OR (highlighted in gray).

| Rank CNti | H1 | H2 | H3 | H4 | H5 | H6 | H7 | Source | CInterH | CTotal | NInterH | NTotal |
|---|---|---|---|---|---|---|---|---|---|---|---|---|
| 1 | 0 | 0 | 0 | 0 | 0 | 0 | 0 | active μ-OR | -585.63 | -412.49 | -483.99 | -493.34 |
| 2 | 0 | 0 | 0 | 0 | 0 | 0 | 0 | inactive δ-OR | -568.50 | -298.47 | -498.05 | -389.21 |
| 3 | 0 | 0 | 0 | 0 | 0 | 0 | 0 | inactive μ-OR | -555.79 | -243.89 | -477.31 | -346.49 |
| 4 | 0 | 0 | 0 | 0 | 0 | 90 | 0 | active μ-OR | -547.59 | -275.92 | -445.12 | -381.11 |
| 5 | 0 | 0 | 0 | 0 | 30 | 0 | 0 | inactive δ-OR | -557.87 | -212.57 | -458.30 | -321.67 |
| 6 | -30 | 0 | 0 | 0 | 0 | 0 | 0 | active μ-OR | -530.57 | -278.27 | -435.89 | -375.60 |
| 7 | 0 | 0 | 0 | 0 | 180 | 180 | 0 | active μ-OR | -533.37 | -250.65 | -433.39 | -359.27 |
| 8 | 0 | 0 | 0 | 0 | 180 | 0 | 0 | inactive δ-OR | -540.11 | -213.09 | -457.24 | -323.18 |
| 9 | -90 | 0 | 0 | 0 | 0 | 0 | 0 | active μ-OR | -524.34 | -302.76 | -433.12 | -409.93 |
| 10 | 0 | 0 | 0 | 0 | -60 | 0 | 0 | active μ-OR | -542.71 | -323.47 | -419.39 | -377.76 |

**Table S2.** Top25 predicted active ensembles structures of human mu opioid receptor (μ-OR) from the SuperBiHelix procedure. Four different energies, charged total energy (CTotal), charged interhelical (CInterH), neutral total (NTotal) and neutral interhelical (NInterH) energy, associated with each 7-helix (H) bundles were evaluated and ranked. The wild-type (WT) structures were ordered by the average rank of these four energies (RankCNti). Source (Soc) is from Bihelix (BH) rank in Table S13.

| H1 | H2 | H3 | H4 | H5 | H6 | H7 | H1 | H2 | H3 | H4 | H5 | H6 | H7 | H1 | H2 | H3 | H4 | H5 | H6 | H7 | Soc | WT |
|---|---|---|---|---|---|---|---|---|---|---|---|---|---|---|---|---|---|---|---|---|---|---|
| 0 | 0 | 0 | 0 | 0 | 0 | 0 | 0 | 0 | 0 | -30 | -30 | -15 | 0 | 0 | 0 | 0 | 0 | 15 | -15 | 0 | 3 | 1 |
| 0 | 0 | 0 | 0 | 0 | 0 | 0 | 0 | 0 | 0 | 30 | 0 | 0 | 0 | 0 | 0 | -15 | -15 | 0 | 0 | 0 | 1 | 2 |
| 0 | 0 | 0 | 0 | 0 | 0 | 0 | 0 | 0 | 0 | -15 | 0 | 0 | 0 | 0 | 0 | 0 | 0 | 0 | 0 | 0 | 1 | 3 |
| 0 | 0 | 0 | 0 | 0 | 0 | 0 | 0 | 0 | 0 | -15 | 0 | 0 | 0 | 0 | 0 | -15 | 0 | 0 | 0 | 0 | 1 | 4 |
| 0 | 0 | 0 | 0 | 0 | 0 | 0 | 0 | 0 | 0 | 30 | 0 | -15 | 0 | 0 | 0 | -15 | 0 | 0 | 0 | 0 | 1 | 5 |
| 0 | 0 | 0 | 0 | 0 | 0 | 0 | 0 | 0 | 0 | 30 | -30 | -15 | 0 | 0 | 0 | 0 | 0 | 15 | -15 | 0 | 3 | 6 |
| 0 | 0 | 0 | 0 | 0 | 0 | 0 | 0 | 0 | 0 | 0 | -30 | 0 | 0 | 0 | 0 | 0 | 0 | 15 | 0 | 0 | 3 | 7 |
| 0 | 0 | 0 | 0 | 0 | 0 | 0 | 0 | 0 | 0 | 0 | 0 | 0 | 0 | 0 | 0 | 0 | 0 | 0 | 0 | 0 | 1 | 8 |
| 0 | 0 | 0 | 0 | 0 | 0 | 0 | 0 | 0 | 0 | 0 | 0 | 0 | 0 | 0 | 0 | 0 | 0 | 0 | 0 | 0 | 1 | 9 |
| 0 | 0 | 0 | 0 | 0 | 0 | 0 | 0 | 0 | 0 | -30 | 0 | 0 | 0 | 0 | 0 | 0 | 0 | 0 | 0 | 0 | 1 | 10 |
| 0 | 0 | 0 | 0 | 0 | 0 | 0 | 0 | 0 | 0 | -30 | 0 | -15 | -15 | 0 | 0 | 0 | 0 | 0 | 0 | 0 | 3 | 11 |
| 0 | 0 | 0 | 0 | 0 | 0 | 0 | 0 | 0 | 0 | 30 | 0 | 0 | 0 | 0 | 0 | -15 | 0 | 0 | 0 | 0 | 1 | 12 |
| 0 | 0 | 0 | 0 | 0 | 0 | 0 | 0 | 0 | 0 | 15 | 0 | 0 | 0 | 0 | 0 | -15 | 0 | 0 | 0 | 0 | 1 | 13 |
| 0 | 0 | 0 | 0 | 0 | -10 | 0 | 0 | 0 | 0 | -30 | -30 | -15 | 15 | 0 | 0 | 0 | 0 | 15 | -15 | 0 | 3 | 14 |
| 0 | 0 | 0 | 0 | -10 | 0 | 0 | 0 | 0 | -15 | -15 | -30 | 15 | 0 | 0 | 0 | 0 | 0 | 0 | 0 | 0 | 3 | 15 |
| 0 | 0 | 0 | 0 | 0 | 0 | 0 | 0 | 0 | 0 | 15 | -30 | 0 | 0 | 0 | 0 | 0 | 0 | 15 | 0 | 0 | 3 | 16 |
| 0 | 0 | 0 | 0 | 0 | -10 | 0 | 0 | 0 | 0 | 30 | -30 | 0 | 15 | 0 | 0 | 0 | 0 | 15 | -15 | 0 | 3 | 17 |
| 0 | 0 | 0 | 0 | 0 | -10 | 0 | 0 | 0 | 0 | 15 | -30 | 15 | 15 | 0 | 0 | 0 | 0 | 15 | -15 | 0 | 3 | 18 |
| 0 | 0 | 0 | 0 | 0 | -10 | 0 | 0 | 0 | 0 | 0 | -30 | 0 | 15 | 0 | 0 | 0 | 0 | 15 | -15 | 0 | 3 | 19 |
| 0 | 0 | 0 | 0 | 0 | 0 | 0 | 0 | 0 | 0 | -15 | -30 | 0 | 0 | 0 | 0 | 0 | 0 | 15 | 0 | 0 | 3 | 20 |
| 0 | 0 | 0 | 0 | 0 | 0 | 0 | 0 | 0 | 0 | -30 | -30 | 0 | 0 | 0 | 0 | 0 | 0 | 15 | 0 | 0 | 3 | 21 |
| 0 | 0 | 0 | 0 | -10 | 0 | 0 | 0 | 0 | -15 | -30 | -30 | 15 | 0 | 0 | 0 | 0 | 0 | 0 | 0 | 0 | 3 | 22 |
| 0 | 0 | 0 | 0 | 0 | -10 | 0 | 0 | 0 | 0 | 30 | -30 | -30 | 15 | 0 | 0 | 0 | 0 | 30 | -15 | 0 | 3 | 23 |
| 0 | 0 | 0 | 0 | 0 | 0 | 0 | 0 | 0 | -15 | -15 | -15 | 15 | 0 | 0 | 0 | 0 | 0 | -30 | 0 | 0 | 3 | 24 |
| 0 | 0 | 0 | 0 | 0 | 0 | 0 | 0 | 0 | 0 | -30 | -30 | 0 | 0 | 0 | 0 | 0 | 0 | 30 | 0 | 0 | 3 | 25 |

**Table S3.** H-bonding analysis of Top25 predicted active ensembles structures of human mu opioid receptor (μ-OR) from the SuperBiHelix procedure. The number of inter and total hydrogen bond (HB) and their energies were calculated. The number of active and inactive, and Class A contacts were also calculated.

| rank | # inter HB | # tot HB | Inter HBE | sum HBE | # active | # inactive | # Class A Contacts |
|---|---|---|---|---|---|---|---|
| 1 | 23 | 46 | -61.34 | -146.30 | 0 | 5 | 38 |
| 2 | 21 | 38 | -61.86 | -139.01 | 7 | 0 | 37 |
| 3 | 14 | 33 | -37.64 | -120.62 | 7 | 0 | 39 |
| 4 | 20 | 35 | -53.19 | -124.41 | 6 | 0 | 37 |
| 5 | 20 | 35 | -55.88 | -136.91 | 7 | 0 | 38 |
| 6 | 22 | 44 | -57.70 | -137.77 | 0 | 5 | 38 |
| 7 | 19 | 34 | -50.22 | -91.58 | 0 | 6 | 39 |
| 8 | 15 | 33 | -34.62 | -113.01 | 7 | 0 | 39 |
| 9 | 15 | 33 | -34.62 | -113.01 | 7 | 0 | 39 |
| 10 | 16 | 30 | -40.56 | -109.67 | 7 | 0 | 39 |
| 11 | 18 | 30 | -55.89 | -114.36 | 0 | 6 | 40 |
| 12 | 23 | 39 | -59.36 | -139.94 | 6 | 0 | 38 |
| 13 | 24 | 39 | -58.08 | -138.54 | 6 | 0 | 37 |
| 14 | 25 | 40 | -62.43 | -121.66 | 0 | 2 | 38 |
| 15 | 26 | 40 | -57.36 | -117.40 | 0 | 4 | 38 |
| 16 | 22 | 36 | -54.67 | -90.35 | 0 | 6 | 39 |
| 17 | 23 | 38 | -54.28 | -111.90 | 0 | 3 | 38 |
| 18 | 23 | 37 | -61.14 | -121.11 | 0 | 2 | 38 |
| 19 | 21 | 37 | -51.01 | -109.14 | 0 | 3 | 38 |
| 20 | 21 | 36 | -46.88 | -86.84 | 0 | 6 | 39 |
| 21 | 20 | 35 | -50.55 | -90.49 | 0 | 6 | 39 |
| 22 | 27 | 41 | -56.59 | -116.38 | 0 | 4 | 38 |
| 23 | 21 | 35 | -59.40 | -111.74 | 1 | 3 | 39 |
| 24 | 14 | 25 | -42.46 | -90.22 | 0 | 6 | 39 |
| 25 | 19 | 37 | -46.99 | -103.72 | 0 | 7 | 39 |

**Table S4.** Top10 predicted active ensembles structures of human kappa opioid receptor (κ-OR) from the BiHelix procedure. Four different energies, charged total energy (CTotal), charged interhelical (CInterH), neutral total (NTotal) and neutral interhelical (NInterH) energy, associated with each 7-helix (H) bundles were evaluated and ranked. The structures were ordered by the average rank of these four energies (RankCNti). Chosen 4 conformers for SuperBiHelix sampling are all-zero structures of inactive κ-OR, active μ-OR, partial active κ-OR, and #13 (highlighted in gray).

| Rank CNti | H1 | H2 | H3 | H4 | H5 | H6 | H7 | Source | CInterH | CTotal | NInterH | NTotal |
|---|---|---|---|---|---|---|---|---|---|---|---|---|
| 1 | 0 | 0 | 0 | 0 | 0 | 0 | 0 | inactive κ-OR | -567.60 | -286.29 | -478.62 | -417.01 |
| 2 | 0 | 0 | 0 | 0 | 0 | 0 | 0 | active μ-OR | -565.28 | -195.68 | -461.16 | -340.47 |
| 3 | 0 | 0 | 0 | 0 | 30 | 0 | 0 | inactive κ-OR | -557.73 | -170.69 | -461.31 | -328.68 |
| 4 | 180 | 0 | 0 | 0 | 0 | 0 | 0 | active μ-OR | -567.76 | -164.71 | -453.27 | -310.12 |
| 5 | 0 | 0 | 0 | 0 | -30 | 0 | 0 | inactive κ-OR | -553.67 | -131.88 | -469.10 | -331.09 |
| 6 | 0 | 0 | 0 | 0 | 0 | 0 | 0 | partial active κ-OR | -563.91 | -124.13 | -492.08 | -313.34 |
| 7 | 0 | 0 | 0 | 0 | 90 | 0 | 0 | active μ-OR | -530.24 | -192.57 | -449.57 | -320.34 |
| 8 | 0 | 0 | 0 | 0 | 0 | 0 | 0 | inactive μ-OR | -533.51 | -155.51 | -456.25 | -296.89 |
| 9 | -120 | 0 | 0 | 0 | 0 | 0 | 0 | active μ-OR | -552.57 | -160.87 | -430.88 | -299.79 |
| 10 | 90 | 0 | 0 | 0 | 0 | 0 | 0 | inactive κ-OR | -522.19 | -216.94 | -428.90 | -371.70 |
| 11 | -90 | 0 | 0 | 0 | 0 | 0 | 0 | mOPRMAg | -531.88 | -144.47 | -428.99 | -301.31 |
| 12 | 0 | 0 | 0 | 0 | 120 | 0 | 0 | mOPRMAg | -507.17 | -162.73 | -437.53 | -303.06 |
| 13 | 0 | 0 | 0 | 0 | 30 | 90 | 0 | hOPRK | -519.90 | -87.35 | -458.02 | -312.23 |
| 14 | 0 | 0 | 0 | 0 | 30 | -30 | 0 | hOPRK | -534.26 | -86.28 | -446.01 | -275.20 |
| 15 | 0 | 0 | 0 | -30 | 30 | 0 | 0 | hOPRK | -549.35 | -120.83 | -447.45 | -243.95 |
| 16 | 0 | 0 | 0 | 0 | 0 | 90 | 0 | mOPRMAg | -514.36 | -126.47 | -422.63 | -312.89 |
| 17 | 0 | 0 | -30 | 0 | 0 | 0 | 0 | hOPRK | -506.77 | -160.39 | -424.22 | -300.88 |
| 18 | 0 | 0 | 0 | 0 | -150 | -90 | 0 | mOPRMAg | -522.99 | -108.89 | -433.28 | -254.42 |
| 19 | 0 | 0 | 0 | 30 | 0 | 0 | 0 | hOPRK | -508.45 | -137.63 | -416.63 | -318.17 |
| 20 | 0 | 0 | 0 | 0 | 90 | 90 | 0 | mOPRMAg | -536.38 | -99.39 | -438.67 | -244.46 |

**Table S5.** Top25 predicted active ensembles structures of human kappa opioid receptor (κ-OR) from the SuperBiHelix procedure. Four different energies, charged total energy (CTotal), charged interhelical (CInterH), neutral total (NTotal) and neutral interhelical (NInterH) energy, associated with each 7-helix (H) bundles were evaluated and ranked. The active wild-type (WT') structures were ordered by the average rank of these four energies (RankCNti). Source (Soc) is from Bihelix (BH) rank in Table S4

.

| H1 | H2 | H3 | H4 | H5 | H6 | H7 | H1 | H2 | H3 | H4 | H5 | H6 | H7 | H1 | H2 | H3 | H4 | H5 | H6 | H7 | Soc | WT' |
|---|---|---|---|---|---|---|---|---|---|---|---|---|---|---|---|---|---|---|---|---|---|---|
| **0** | 0 | 0 | 0 | 0 | 0 | 0 | 0 | 0 | 0 | -15 | 0 | 15 | 0 | 0 | 0 | 0 | -15 | 0 | 0 | 0 | 2 | 1 |
| **0** | 0 | 0 | 0 | 0 | 0 | 0 | 0 | 0 | 0 | 0 | 0 | 15 | 0 | 0 | 0 | 0 | 0 | 0 | 0 | 0 | 2 | 2 |
| **0** | 0 | 0 | 0 | 0 | 0 | 0 | 0 | 0 | 0 | 0 | 0 | 0 | 0 | 0 | 0 | 0 | -15 | 0 | 0 | 0 | 2 | 3 |
| **0** | 0 | 0 | 0 | 0 | 0 | 0 | 0 | 0 | 0 | 0 | 0 | 30 | 0 | 0 | 0 | 0 | -15 | 0 | 0 | 0 | 2 | 4 |
| **0** | 0 | 0 | 0 | 0 | 0 | 0 | 0 | 0 | 0 | 0 | 0 | 0 | 0 | 0 | 0 | -15 | 0 | 0 | 0 | 0 | 2 | 5 |
| **0** | 0 | 0 | 0 | 0 | 0 | 0 | 0 | 0 | 0 | -15 | 0 | 30 | 0 | 0 | 0 | 0 | -15 | 0 | 0 | 0 | 2 | 6 |
| **0** | 0 | 0 | 0 | 0 | 0 | 0 | 0 | 0 | 0 | 0 | -15 | 0 | 0 | 0 | 0 | 0 | -15 | 0 | 0 | 0 | 2 | 7 |
| **0** | 0 | 0 | 0 | 10 | 0 | 0 | 0 | 0 | 0 | 30 | -15 | -15 | 0 | 0 | 0 | -15 | -15 | 15 | 0 | 0 | 2 | 8 |
| **0** | 0 | 0 | 0 | 0 | 0 | 0 | 0 | 0 | 0 | 30 | 0 | 15 | 0 | 0 | 0 | 0 | 0 | 0 | 0 | 0 | 2 | 9 |
| **0** | 0 | 0 | 0 | 0 | 0 | 0 | 0 | 0 | 0 | 30 | 0 | 0 | 0 | 0 | 0 | -15 | -15 | 0 | 0 | 0 | 2 | 10 |
| **0** | 0 | 0 | 0 | 0 | 0 | 0 | 0 | 0 | 0 | -30 | 0 | 0 | 0 | 0 | 0 | -15 | 0 | 0 | 0 | 0 | 2 | 11 |
| **0** | 0 | 0 | 0 | 0 | 0 | 0 | 0 | 0 | 0 | 30 | -15 | 15 | 0 | 0 | 0 | 0 | 0 | 0 | 0 | 0 | 2 | 12 |
| **0** | 0 | 0 | 0 | 0 | 0 | 0 | 0 | 0 | 0 | -15 | 0 | 0 | 0 | 0 | 0 | 0 | -15 | 0 | 0 | 0 | 2 | 13 |
| **0** | 0 | 0 | 0 | 0 | 0 | 0 | 0 | 0 | 0 | 0 | -15 | 15 | 0 | 0 | 0 | 0 | -15 | 0 | 0 | 0 | 2 | 14 |
| **0** | 0 | 0 | 0 | 0 | 0 | 0 | 0 | 0 | 0 | -15 | 0 | 15 | 0 | 0 | 0 | 0 | 0 | 0 | 0 | 0 | 2 | 15 |
| **0** | 0 | 0 | 0 | 0 | 0 | 0 | 0 | 0 | 0 | 15 | 0 | 0 | 0 | 0 | 0 | -15 | 0 | 0 | 0 | 0 | 2 | 16 |
| **0** | 0 | 0 | 0 | 0 | 0 | 0 | 0 | 0 | 0 | 30 | -15 | 0 | 0 | 0 | 0 | 0 | 0 | 0 | 0 | 0 | 2 | 17 |
| **0** | 0 | 0 | 0 | 0 | -10 | 0 | 0 | 0 | 0 | 0 | 0 | 15 | 30 | 0 | 0 | 0 | 0 | 0 | -15 | 0 | 13 | 18 |
| **0** | 0 | 0 | 0 | 10 | -10 | 0 | 0 | 0 | 0 | 15 | 0 | -30 | 30 | 0 | 0 | -15 | 0 | -15 | -30 | 0 | 13 | 19 |
| **0** | 0 | 0 | 0 | 0 | 0 | 0 | 0 | 0 | 0 | 30 | 0 | 0 | 0 | 0 | 0 | -15 | 0 | 0 | 0 | 0 | 2 | 20 |
| **0** | 0 | 0 | 0 | 0 | 0 | 0 | 0 | 0 | 0 | 15 | 0 | 30 | 0 | 0 | 0 | 0 | 0 | 0 | 0 | 0 | 2 | 21 |
| **0** | 0 | 0 | 0 | 10 | -10 | 0 | 0 | 0 | 0 | 15 | 0 | -15 | 30 | 0 | 0 | -15 | 0 | -15 | -30 | 0 | 13 | 22 |
| **0** | 0 | 0 | 0 | 0 | 0 | 0 | 0 | 0 | 0 | 30 | 0 | 0 | 0 | 0 | 0 | 0 | 0 | 0 | 0 | 0 | 2 | 23 |
| **0** | 0 | 0 | 0 | 0 | -10 | 0 | 0 | 0 | 0 | -15 | 0 | 15 | 30 | 0 | 0 | 0 | 0 | 0 | -15 | 0 | 13 | 24 |
| **0** | 0 | 0 | 0 | 0 | 0 | 0 | 0 | 0 | 0 | -15 | 0 | 0 | 0 | 0 | 0 | -15 | 0 | 0 | 0 | 0 | 2 | 25 |

**Figure S1.** The dose-response activation of human mu opioid receptor by compound **4.** The data was normalized compare to DAMGO.

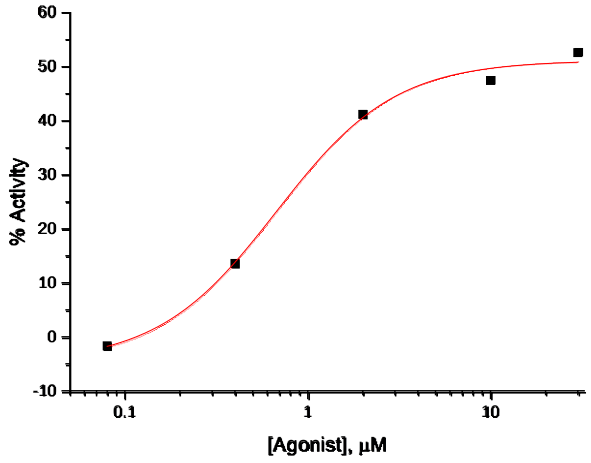

**Figure S2**. (Left) Binding site of Compound **13** at μ-OR and (Right) 2D ligand interaction diagram. The H-bond is represented by the arrows between the donor and the acceptor. Residues within 4 Å of ligand are shown on the 2D ligand interaction diagram displayed on the right. For clarity, only polar hydrogen atoms are shown.

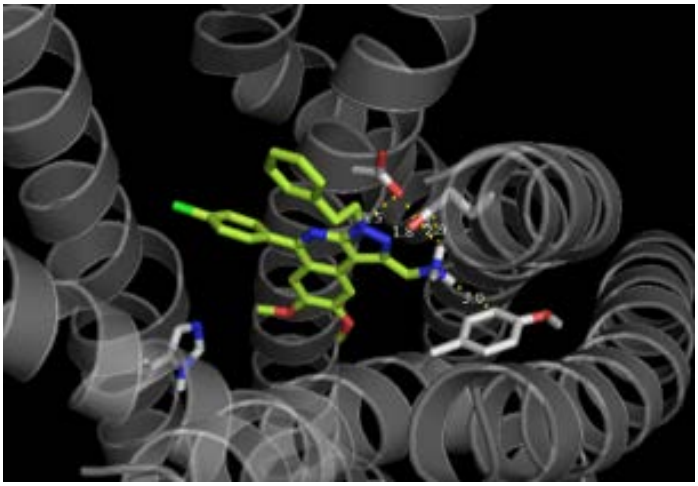

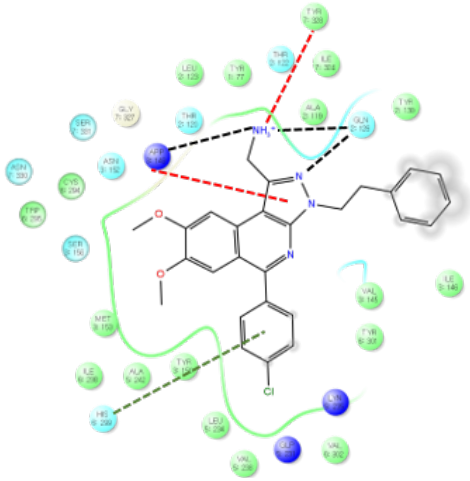

**Figure S3**. Structure of 56 groups at R2 for R-group screening based on ortho Cl substituent at R1 of compound **13**.

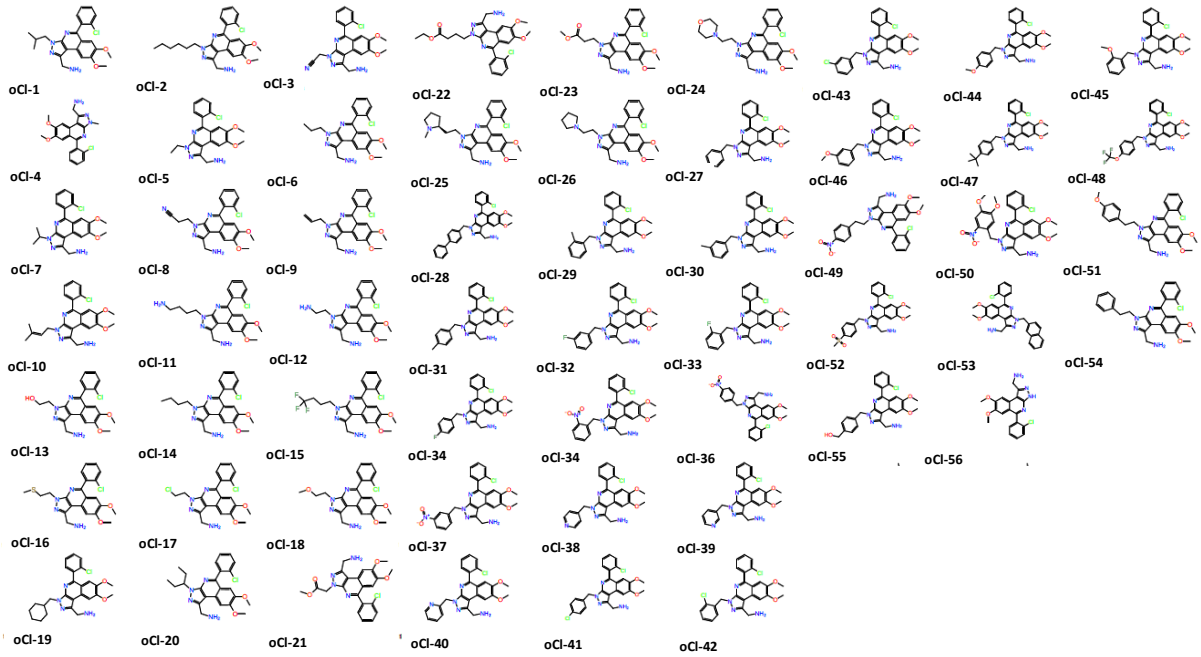

## 1. Computational Methods

### 1.1 The DarwinDock Method for Predicting Ligand-Protein Structures

To predict the optimum ligand binding site to each of the 24 protein conformations from the GEnSeMBLE procedure, we used the DarwinDock method, which has previously been used to predict ligand-protein structures for many GPCRs.[1]

#### 1.1.1 Selecting Ligand Conformations

Starting from the X-ray structure of each ligand, we sampled the torsion angles of all rotatable bonds to generate multiple conformations for each ligand. These were minimized using Maestro with 10 to 20 ligand conformations selected by energy and diversity. The charges on the ligands were chosen to be the Mulliken charges from density functional theory (B3LYP using the 6-311G** basis set).

#### 1.1.2 Scanning the Receptor for Potential Binding Regions

For each of the 24 protein conformations, the whole protein was alanized (replacing the 6 hydrophobic residues, I, L, V, F, Y, and W with A). Then for each of the 10-20 ligand conformations, we scanned for potential binding regions with no assumption about the binding site. The entire molecular surface was mapped with spheres representing the empty volume of the protein. These spheres were partitioned using the BoxSpheres.pl script to generate 10 Å cubic boxes for each protein conformation. This led to a minimum of 73 boxes for WT13 and a maximum of 83 for WT24 (the WT number from the SuperBiHelix analysis is in Table S1). We then used DOCK4.0[70] to generate 1000 poses for each of these 73-83 regions and selected the most promising three or four putative binding regions for docking.

## 2. Generating the active ensembles for κ-OR

To understand the activation of μ-OR by compound **4**, we used the GEnSeMBLE complete sampling method to generate the ensemble of 24 structures for human μ-OR and κ-OR. [2] As TM templates, we used crystal structures of μ -OR activated structures: BU72 agonist bound mouse μ -OR (PDB ID code 5C1M)[3] κ -OR inactivated structures: antagonist JDTic bound to human κ -OR (PDB ID code 4DJH),[37] antagonist morphinan mouse bonded to μ-OR (PDB ID code 4DKL),[4] antagonist Naltrindole bonded to human δ-OR (PDB ID code 4N6H),[5] peptide mimetic antagonist compound-24 (C-24) bonded human nociceptin receptor (PDB ID code 4EA3),[6] and one partial agonist (EKC) bonded to κ-OR.[51] For each of the 6 templates we carried out the BiHelix analysis for both human μ–OR and κ-OR, examining $6*12^7$ = 220 million packings. Then, we analyzed the predicted packing using the GRoSS active hotspots and the GRoSS inactive hotspots.

### 2.1 κ-OR

**2.1a** BiHelix. As shown in Table S10, 15 of the best 25 are from inactive κ-OR and μ-OR and 10 are from the active μ-OR crystal structure. Thus, 15 show inactive hot spot contacts. To optimize the TM helix tilts along with rotations we carried out SuperBihelix complete sampling for 4 templates from BiHelix selected based on energy and

diversity. For SuperBihelix optimization of tilts and rotations, we selected two X-ray templates (inactive and active μ-OR), one predicted structure (κ-OR bound with partial agonist), and #17 for diversity in Table S10. In the Bihelix predictions, the X-ray template of inactive κ -OR has the most inactive hotspots (7) and the most Class A contacts (40). For the active template, we selected the X-ray template of active μ-OR.

**2.1b** SuperBiHelix for best active

The SuperBihelix considered tilt angles of θ=0,±10°, azimuthal angles of ϕ=0, ±15°, ±30°, and rotation angles of η=0, ±15°, ±30°, for a total of 13 trillion that was reduced to the Top25 based on the packing of the best 7-helix bundles, all from inactive κ-OR. Then we excluded the κ-OR template, and rescored to find that the majority (21 of 25) are from μ-OR active template (Table S5). All Top25 and 19 models have salt-bridges between R3.50-D7.57 and between R5.69-D6.37 which are unique for active ensembles, respectively. But we do not observe any TM 3-5-6 H-bonding networks in blue, which are unique for inactive ensembles (Table S1) except for two cases from inactive κ-OR template (#13). Out of the Top25, 20 are from active μ-OR template and 4 are from inactive κ-OR template (#13). Thus, most structures in the ensemble are expected to be active.

**2.1c** SuperBiHelix for best inactive

Table S4 shows the top25 inactive structures from inactive κ-OR. All show 6 to 7 inactive hot spot interactions.

## 3. Spectroscopy of final compounds

## 1-(5-(3-chlorophenyl)-7,8-dimethoxy-3-(3-methoxybenzyl)-3H-pyrazolo[3,4-c]isoquinolin-1-yl)-N,N-dimethylmethanamine (15)

- Proton NMR of compound 15

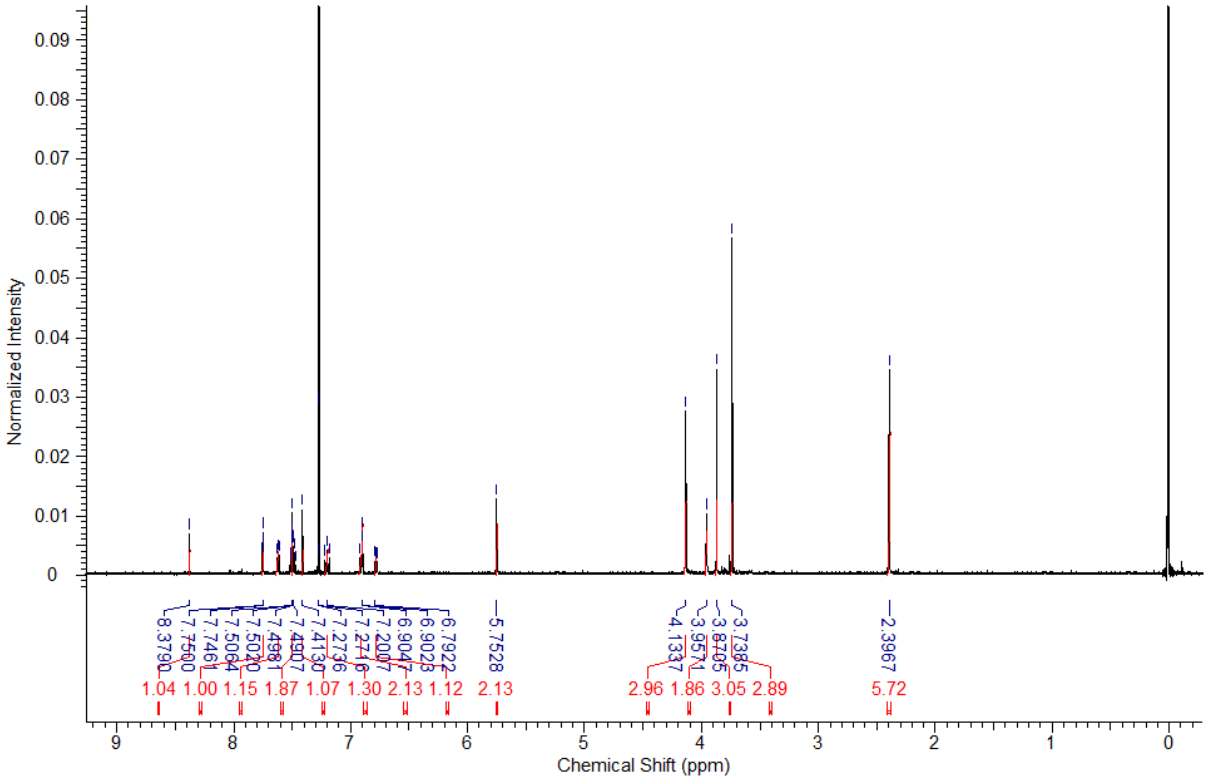


- Carbon NMR of compound 15

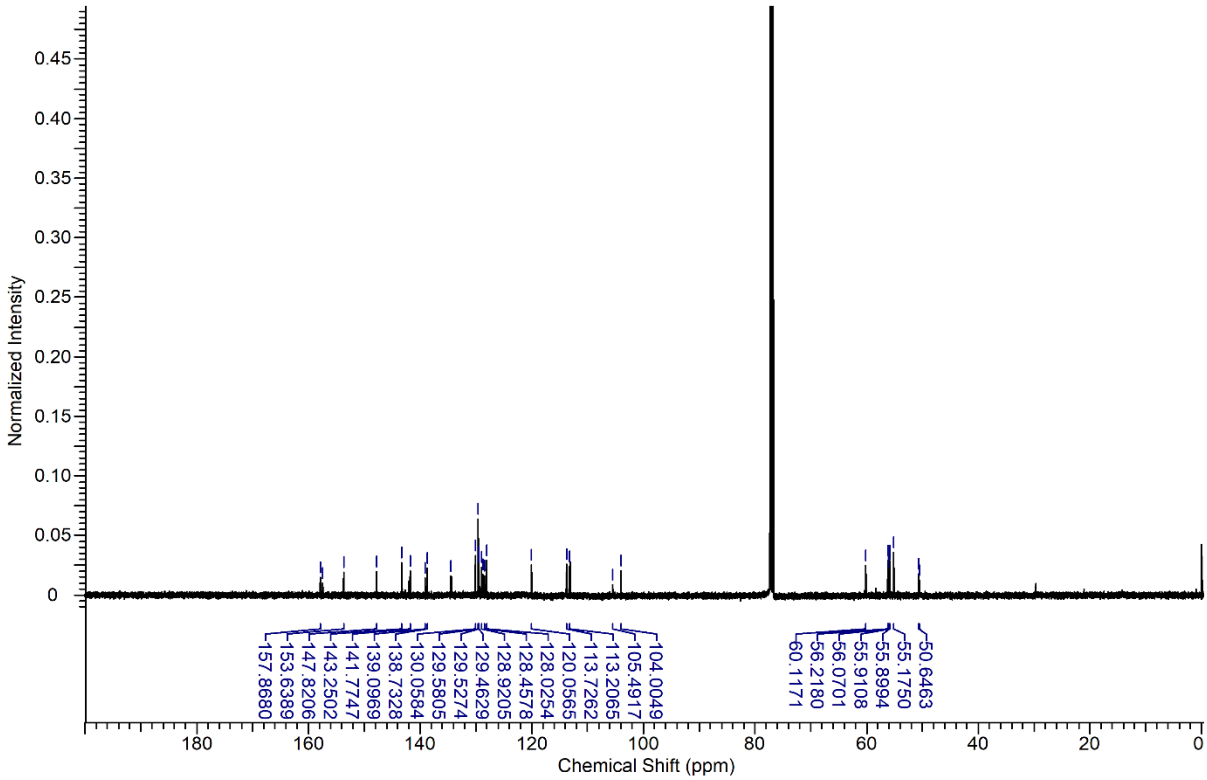

**(5-(3-chlorophenyl)-7,8-dimethoxy-3-(naphthalen-2-ylmethyl)-3H-pyrazolo[3,4-c]isoquinolin-1-yl)methanamine (16)**

- Proton NMR of compound 16

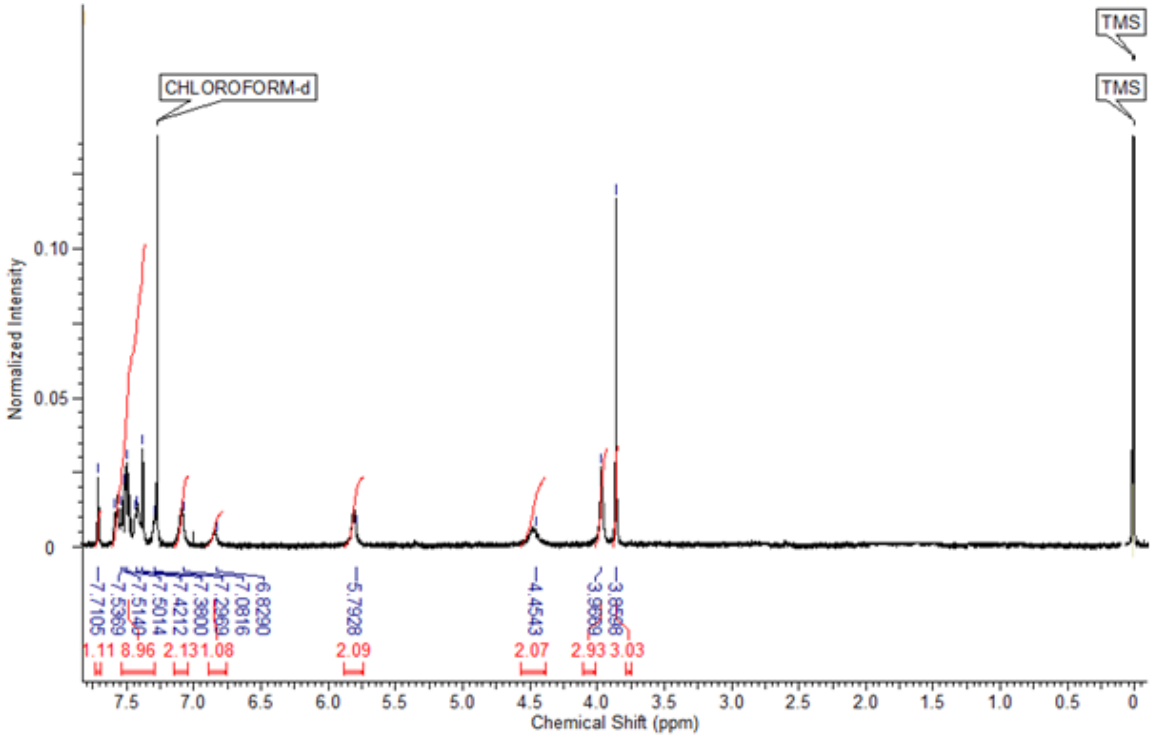


- Carbon NMR of compound 16

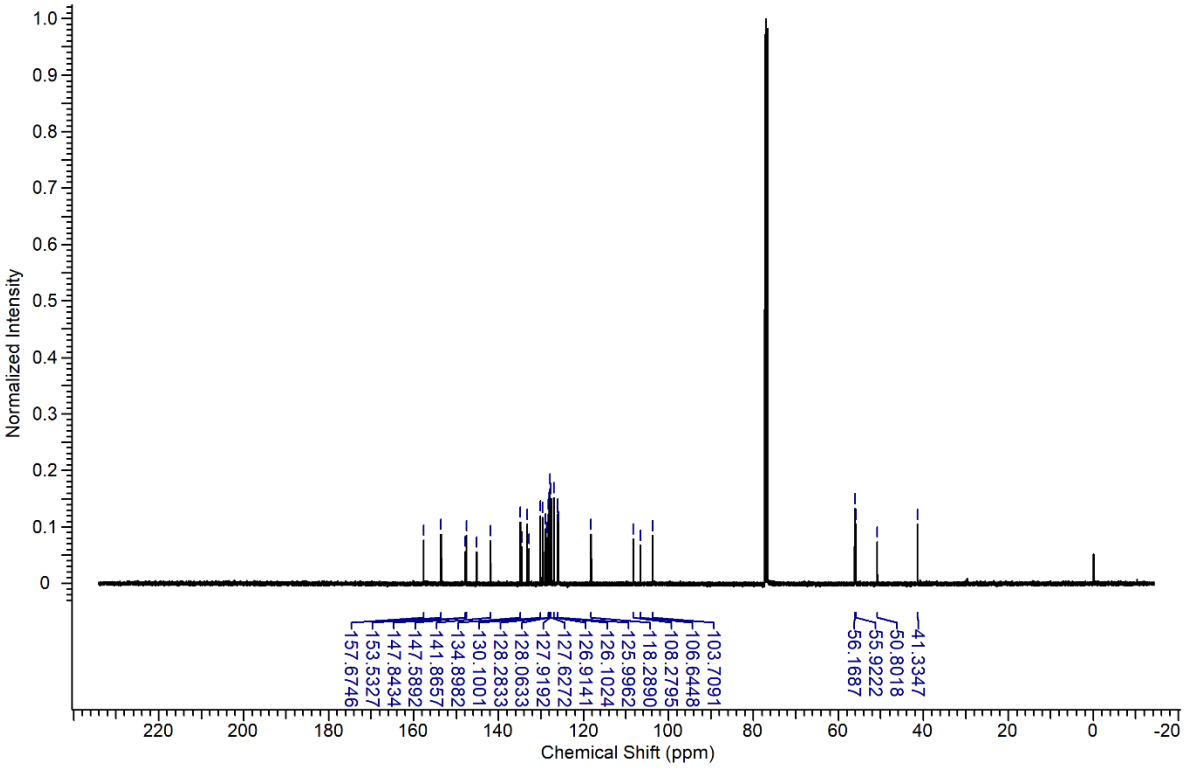

**1-(5-(3-chlorophenyl)-7,8-dimethoxy-3-(4-(methylsulfonyl)benzyl)-3H-pyrazolo[3,4-c]isoquinolin-1-yl)-N,N-dimethylmethanamine (19)**

- Proton NMR of compound 19

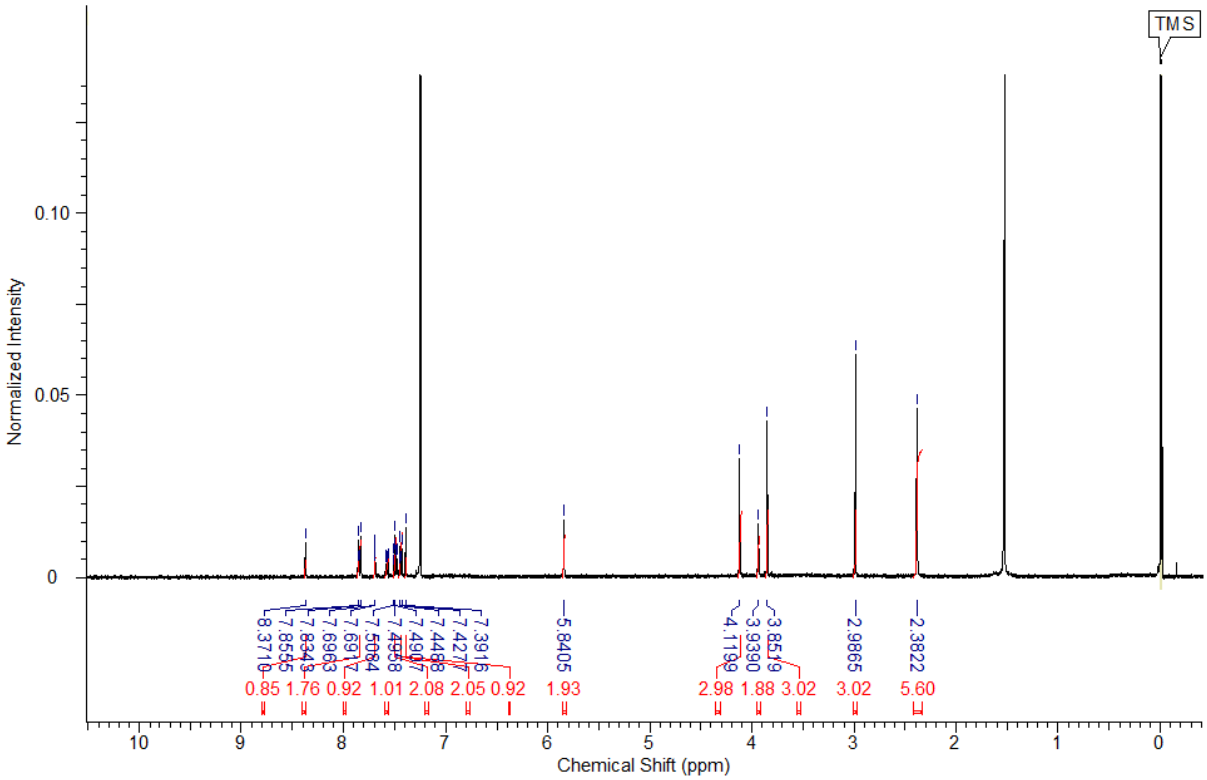


- Carbon NMR of compound 19

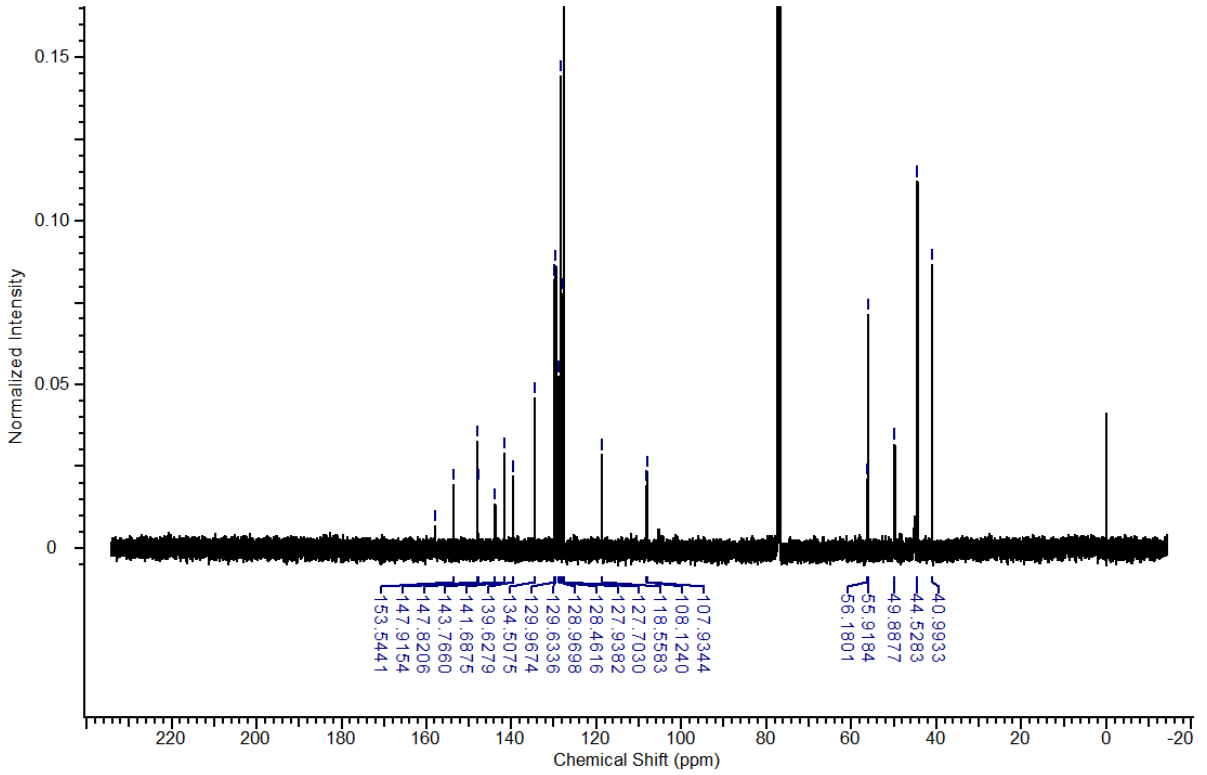

**1-(5-(3-chlorophenyl)-7,8-dimethoxy-3-(naphthalen-2-ylmethyl)-3H-pyrazolo[3,4-c]isoquinolin-1-yl)-N,N-dimethylmethanamine (20)**

- Proton NMR of compound 20

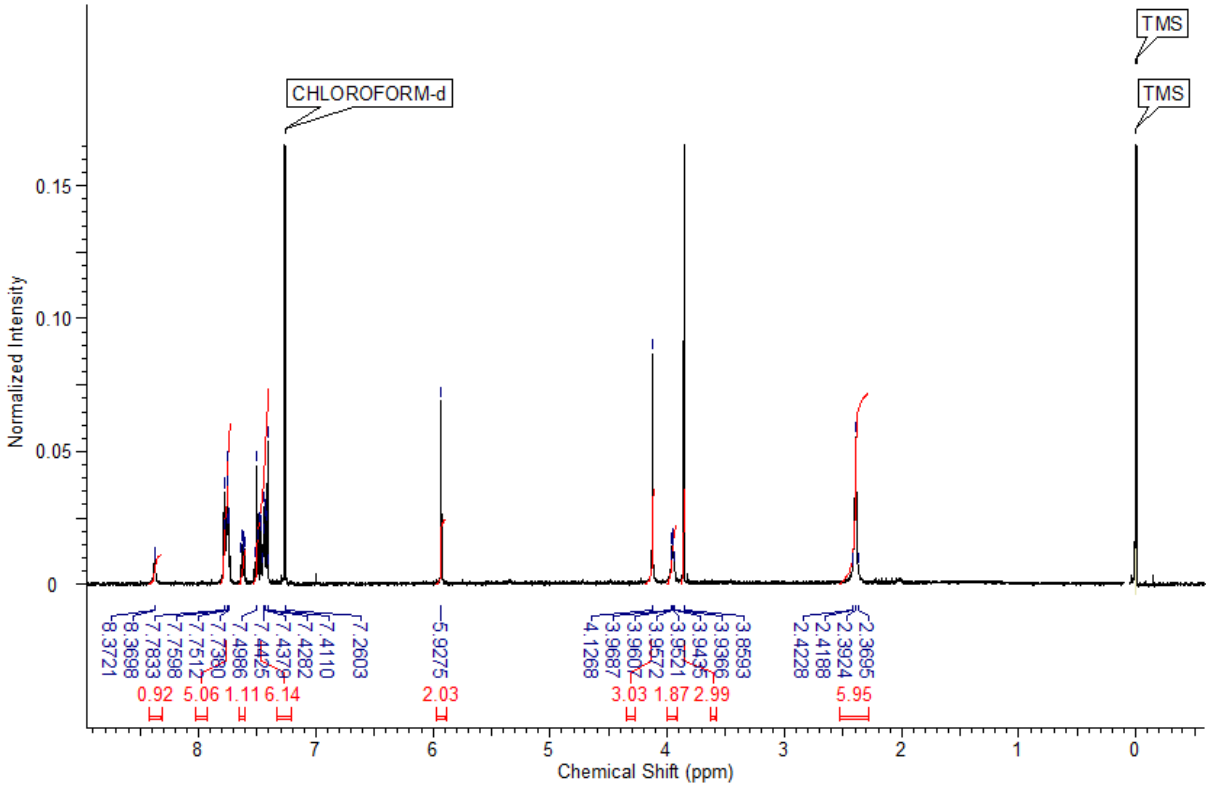


- Carbon NMR of compound 20

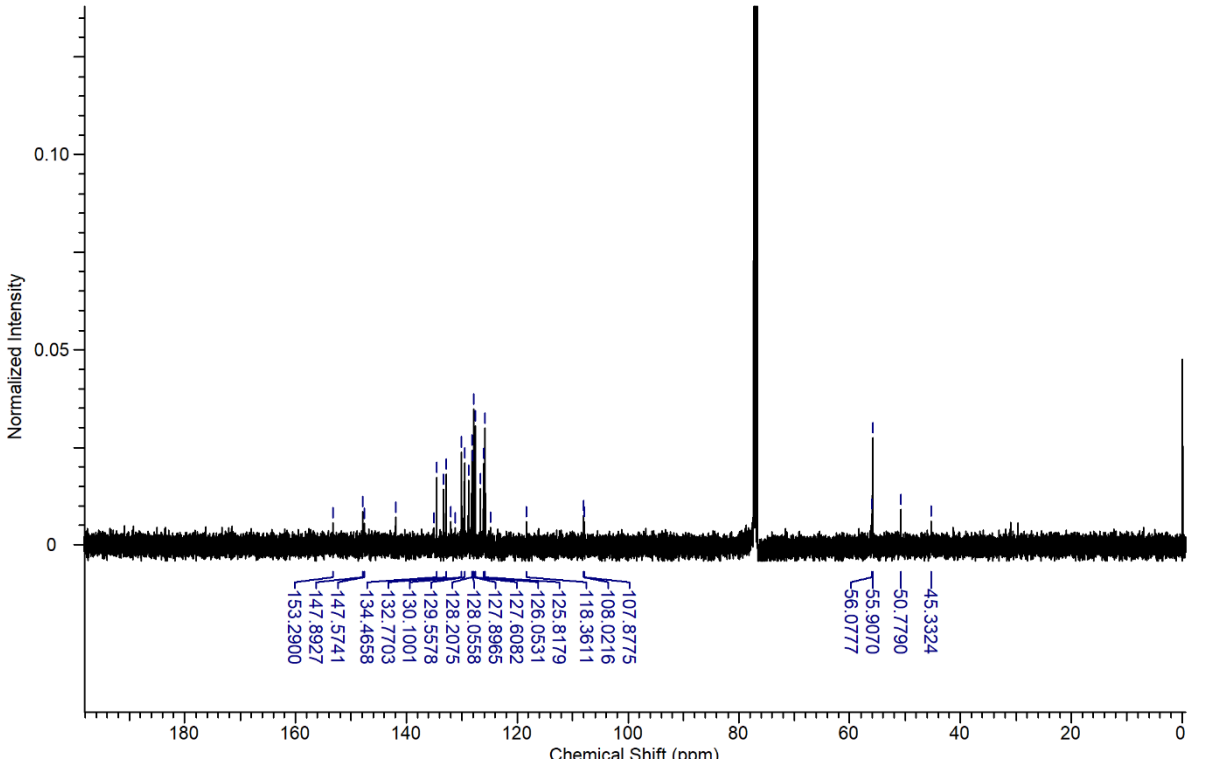

**1-(5-(4-chlorophenyl)-7,8-dimethoxy-3-(naphthalen-2-ylmethyl)-3H-pyrazolo[3,4-c]isoquinolin-1-yl)methanamine (22)**

- Proton NMR of compound 22

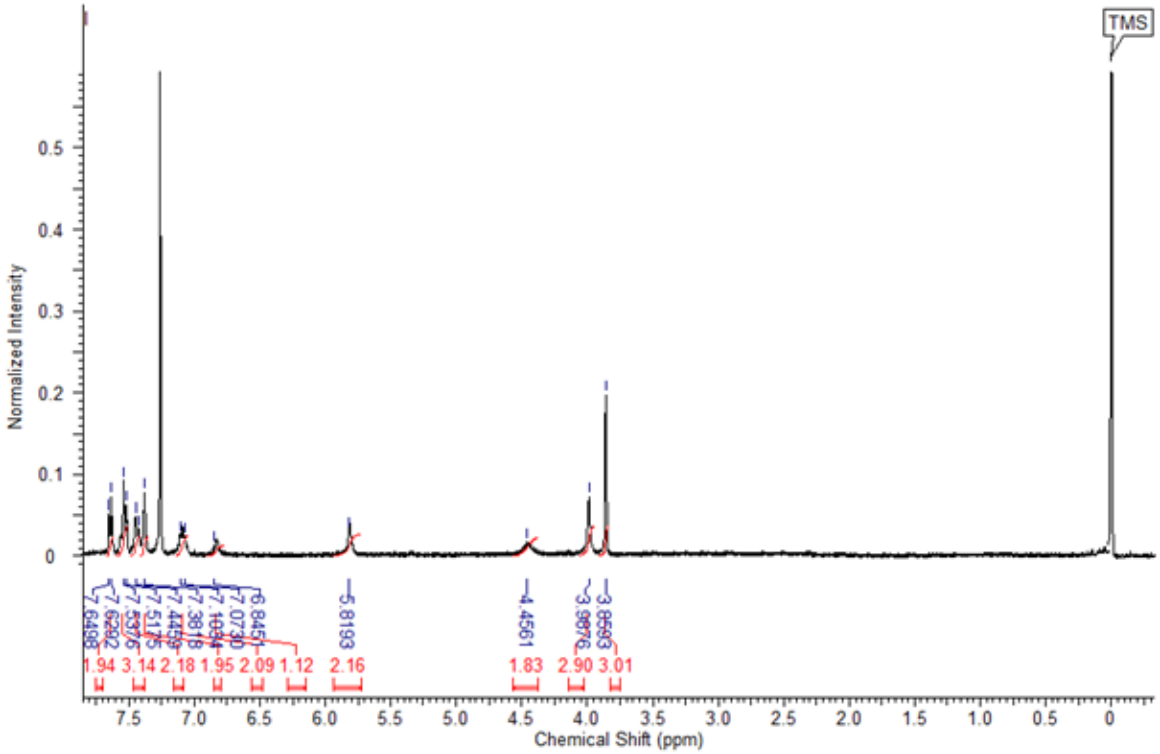


- Carbon NMR of compound 22

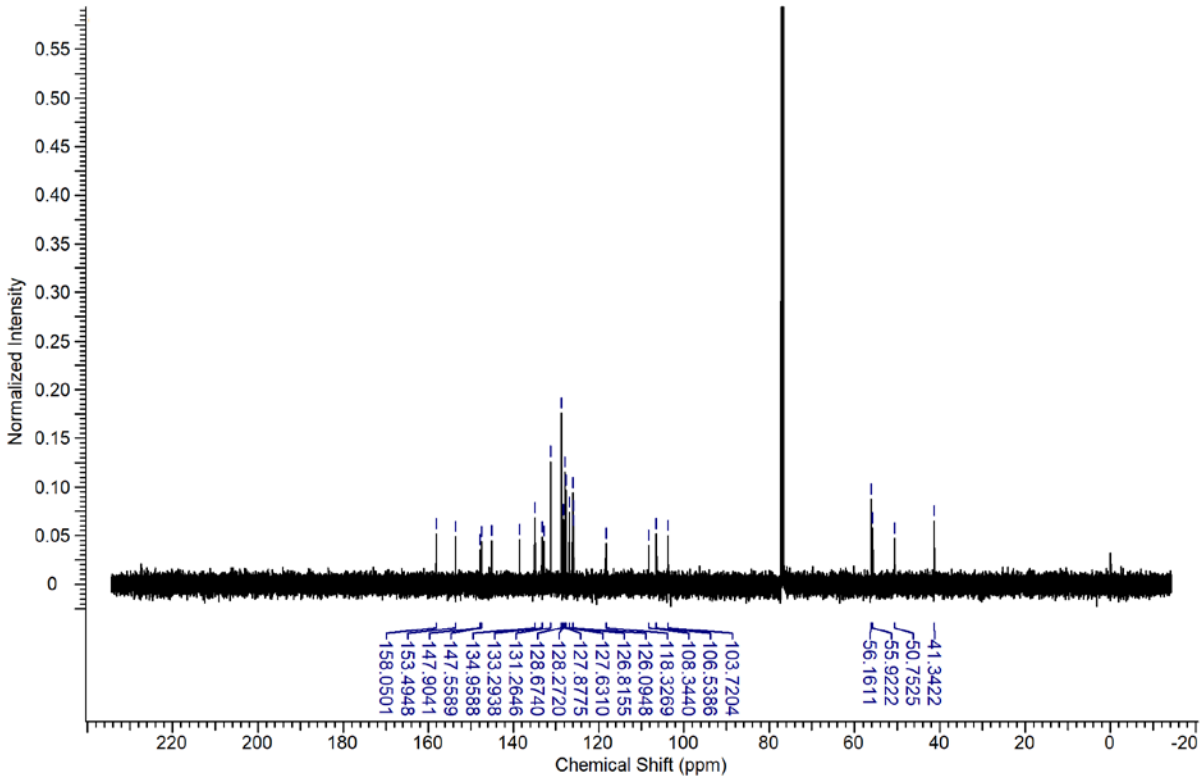

**1-(5-(3-chlorophenyl)-7,8-dimethoxy-3-(4-methoxyphenethyl)-3H-pyrazolo[3,4-c]isoquinolin-1-yl)-N,N-dimethylmethanamine (25)**

- Proton NMR of compound 25

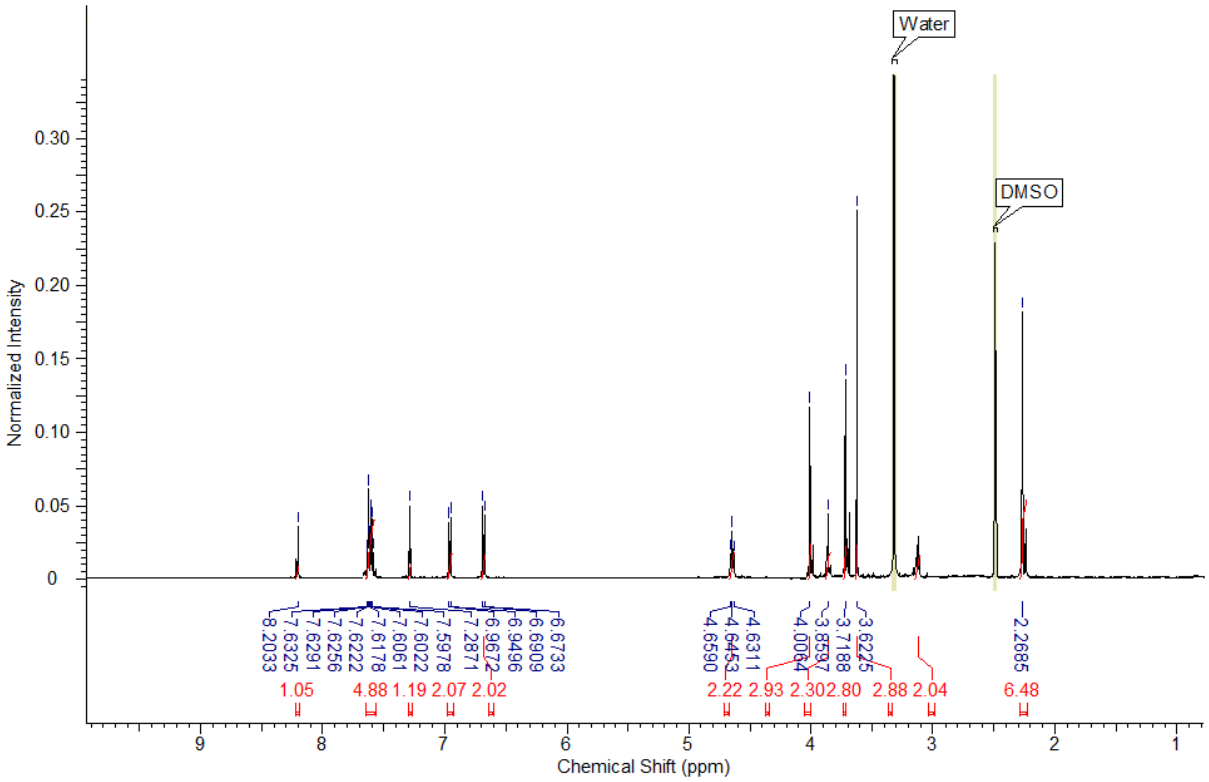


- Carbon NMR of compound 25

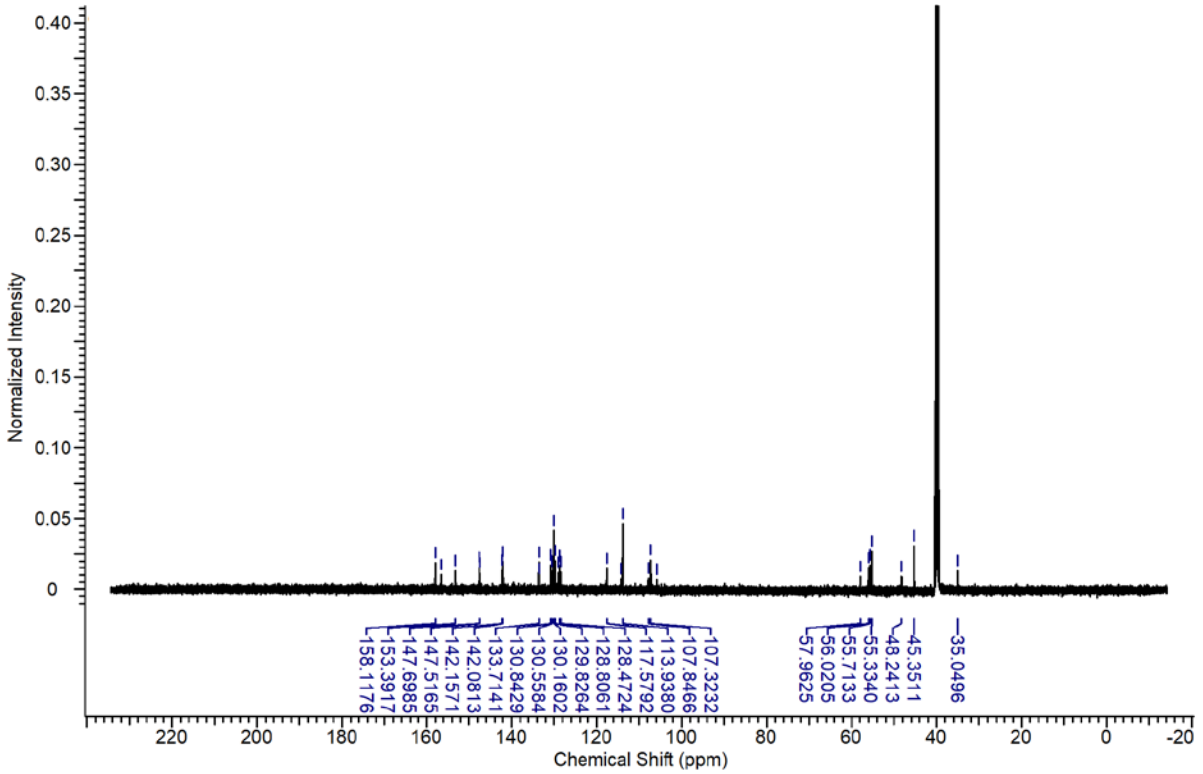

**1-(5-(4-chlorophenyl)-3-isobutyl-7,8-dimethoxy-3H-pyrazolo[3,4-c]isoquinolin-1-yl)-N,N-dimethylmethanamine (26)**

- Proton NMR of compound 26

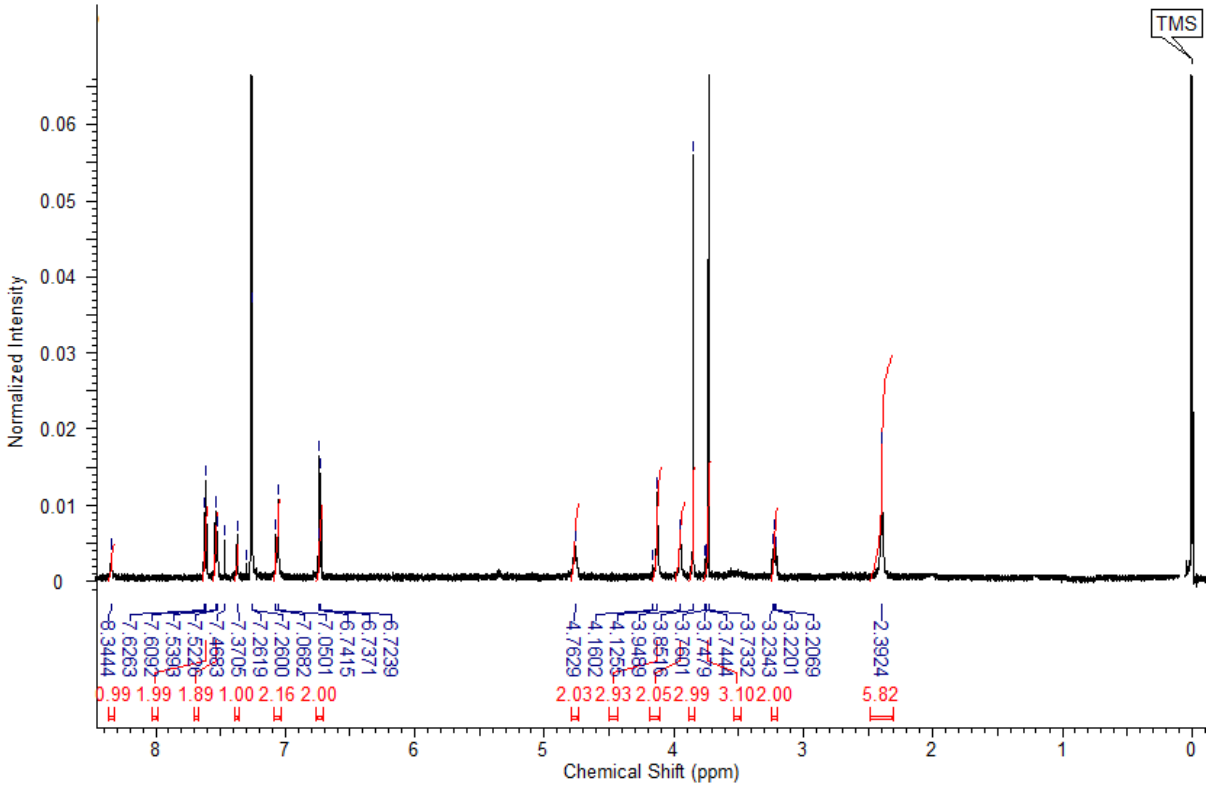


- Carbon NMR of compound 26

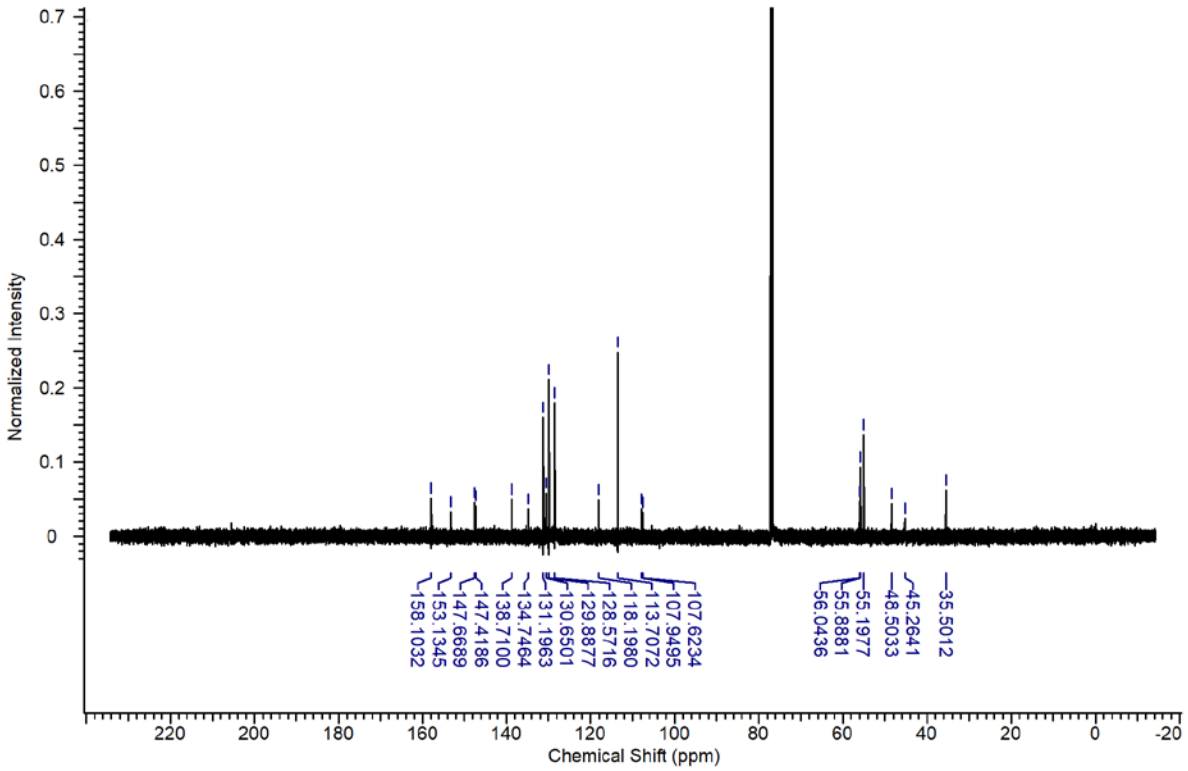

**1-(5-(2-chlorophenyl)-7,8-dimethoxy-3-(4-methoxyphenethyl)-3H-pyrazolo[3,4-c]isoquinolin-1-yl)-N,N-dimethylmethanamine (27)**

- Proton NMR of compound 27

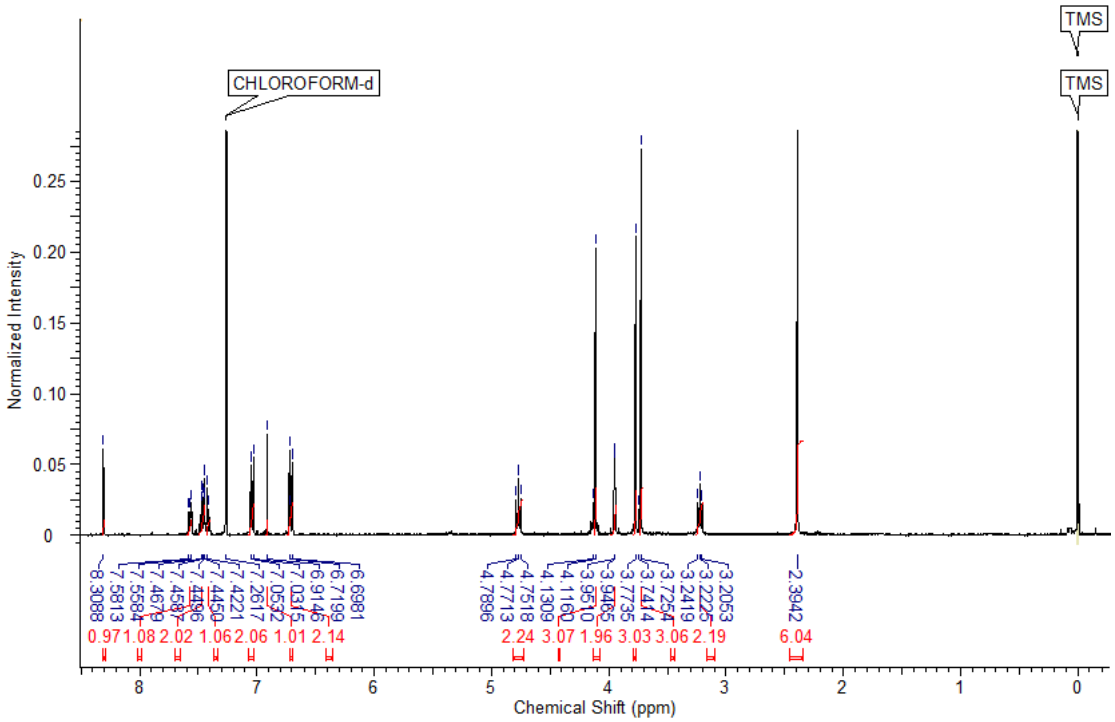


- Carbon NMR of compound 27

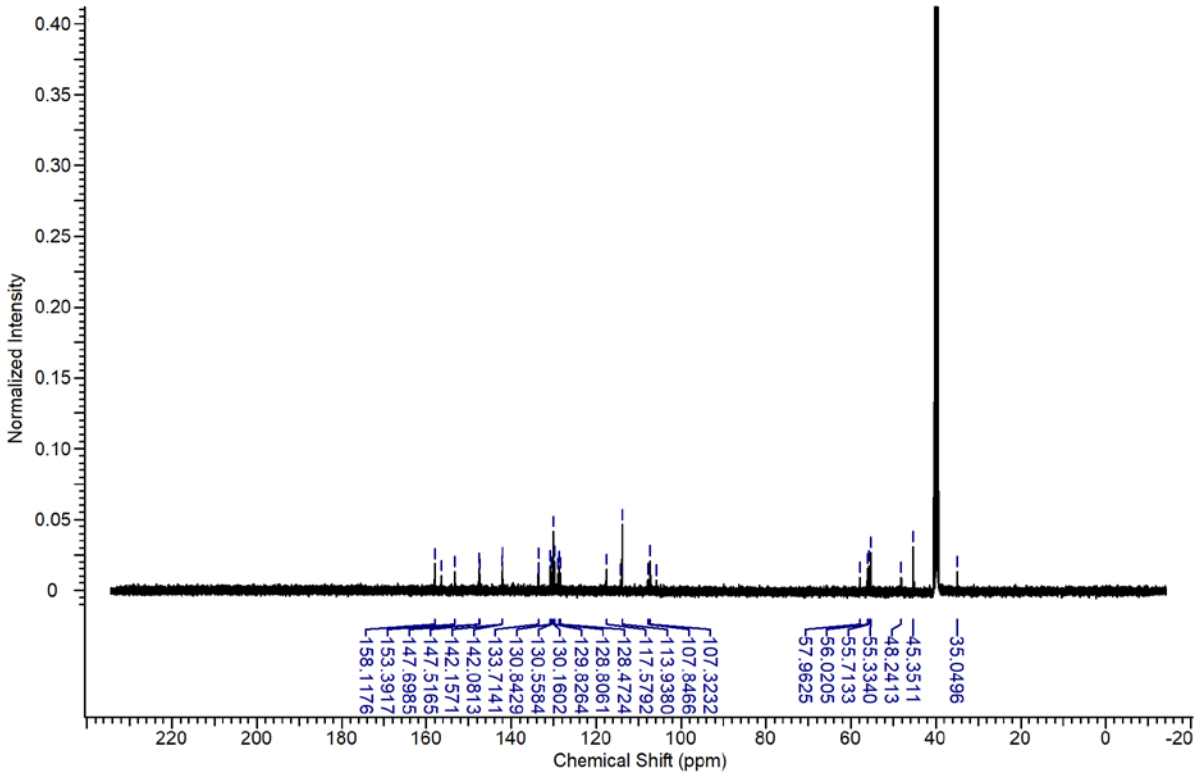

**3-(5-(3-chlorophenyl)-1-((dimethylamino)methyl)-7,8-dimethoxy-3H-pyrazolo[3,4-c]isoquinolin-3-yl)propanenitrile (29)**

- Proton NMR of compound 29

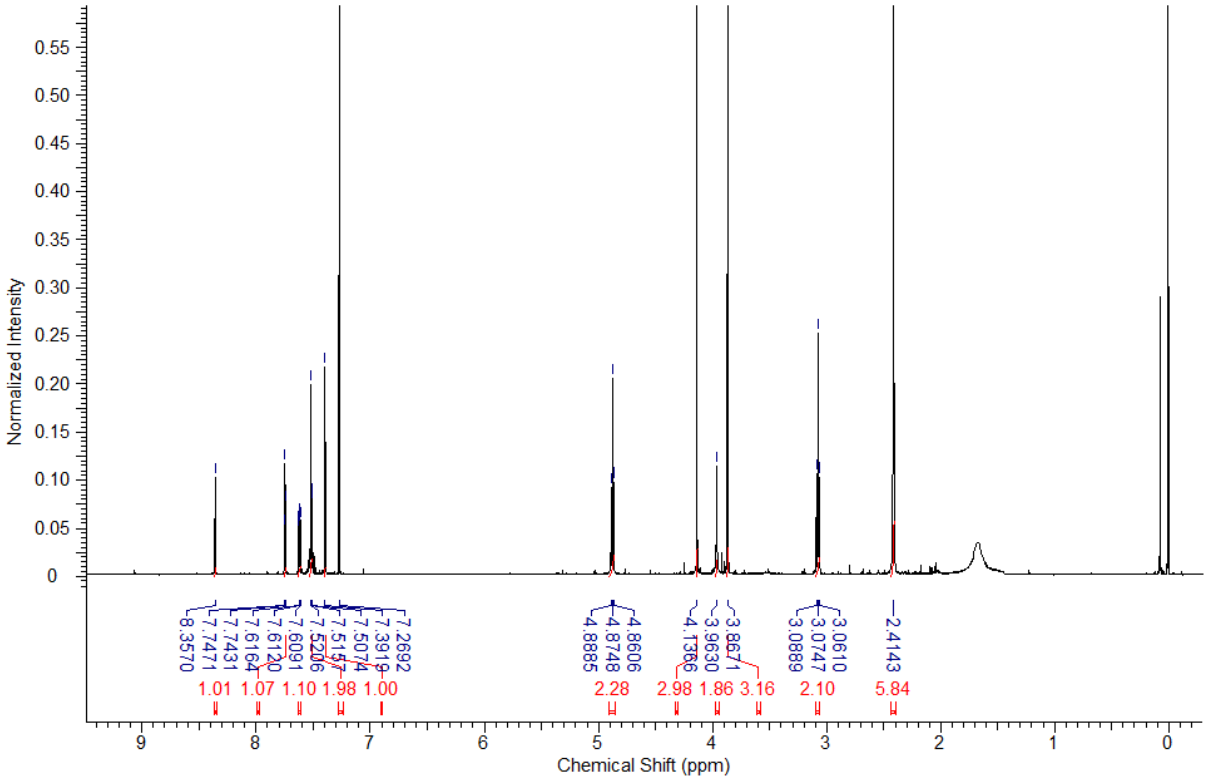


- Carbon NMR of compound 29

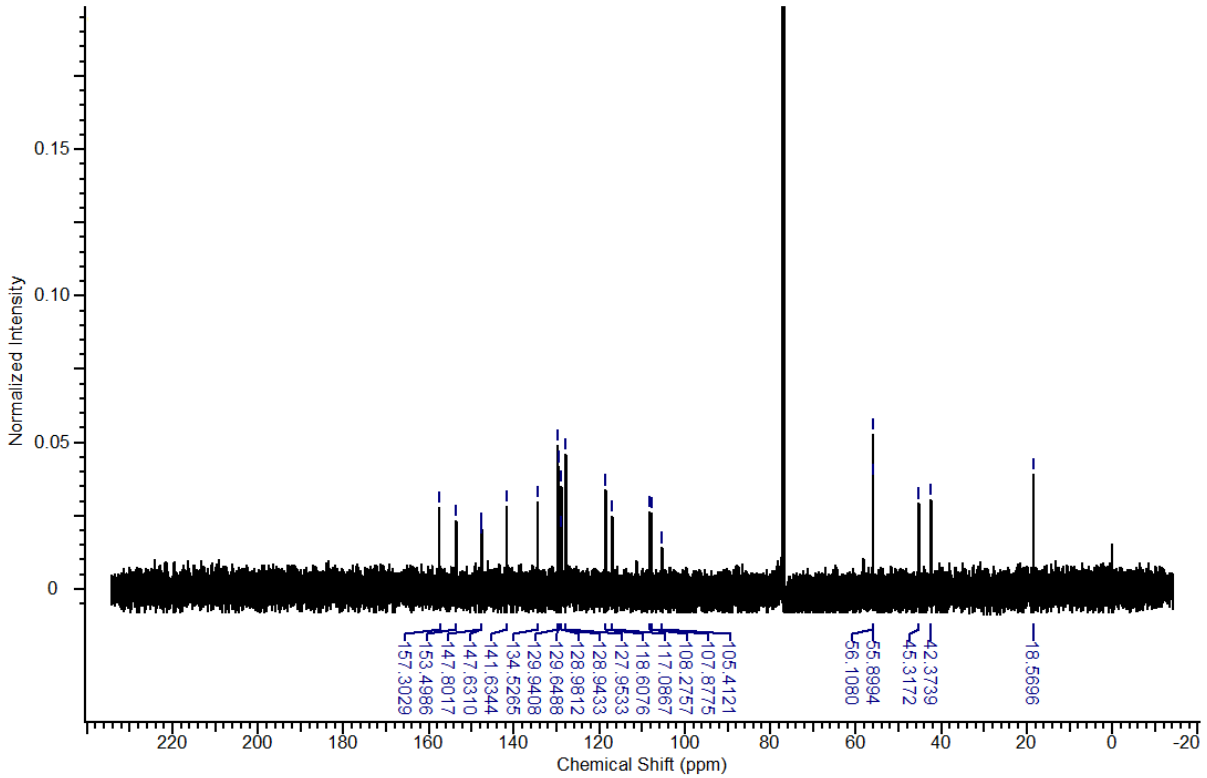

**1-(5-(3-chlorophenyl)-3-isobutyl-7,8-dimethoxy-3H-pyrazolo[3,4-c]isoquinolin-1-yl)-N,N-dimethylmethanamine (30)**

- Proton NMR of compound 30

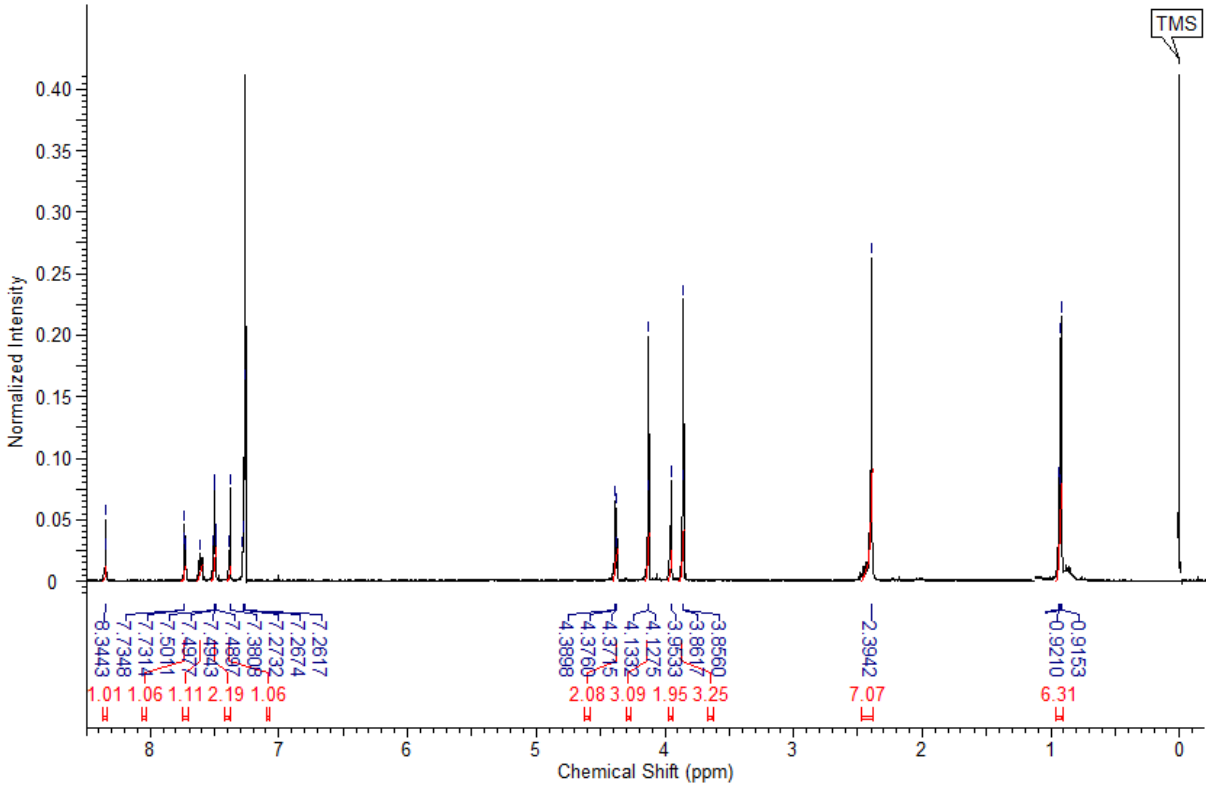


- Carbon NMR of compound 30

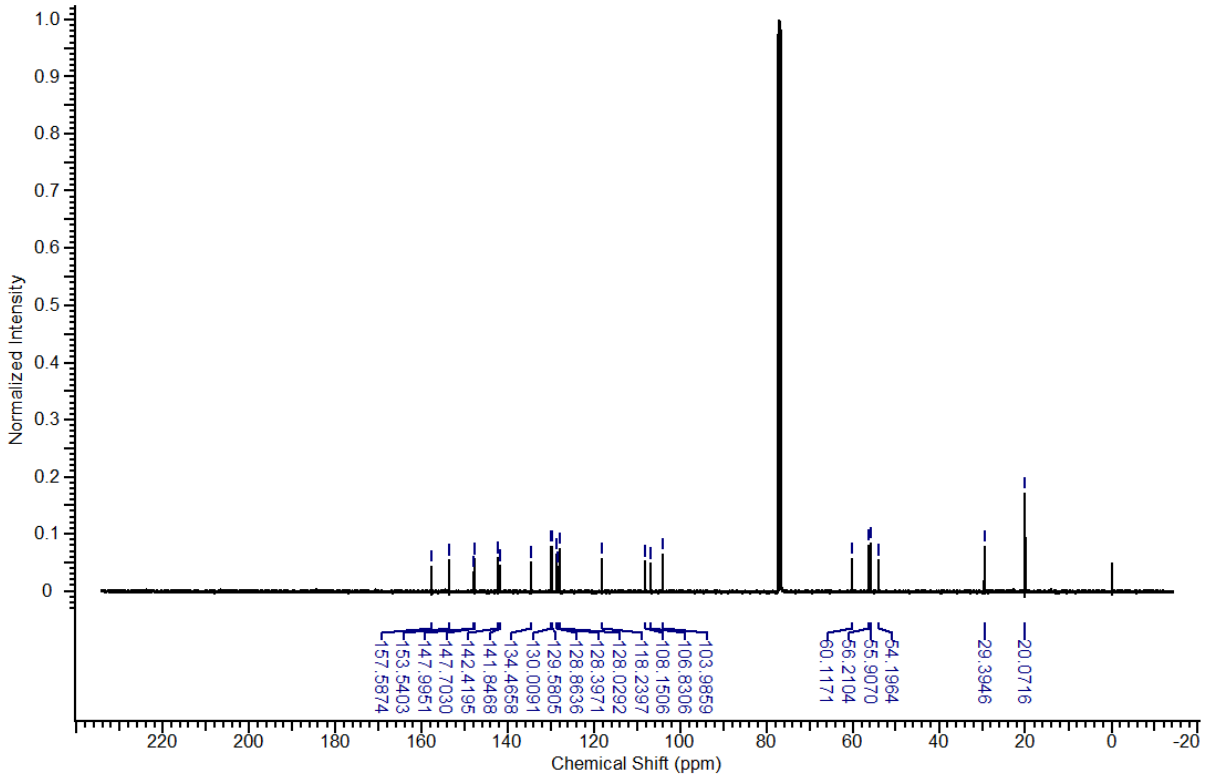

## 1-(5-(3-chlorophenyl)-7,8-dimethoxy-3-(2-(1-methylpyrrolidin-2-yl)ethyl)-3H-pyrazolo[3,4-c]isoquinolin-1-yl)-N,N-dimethylmethanamine (31)

- Proton NMR of compound 31

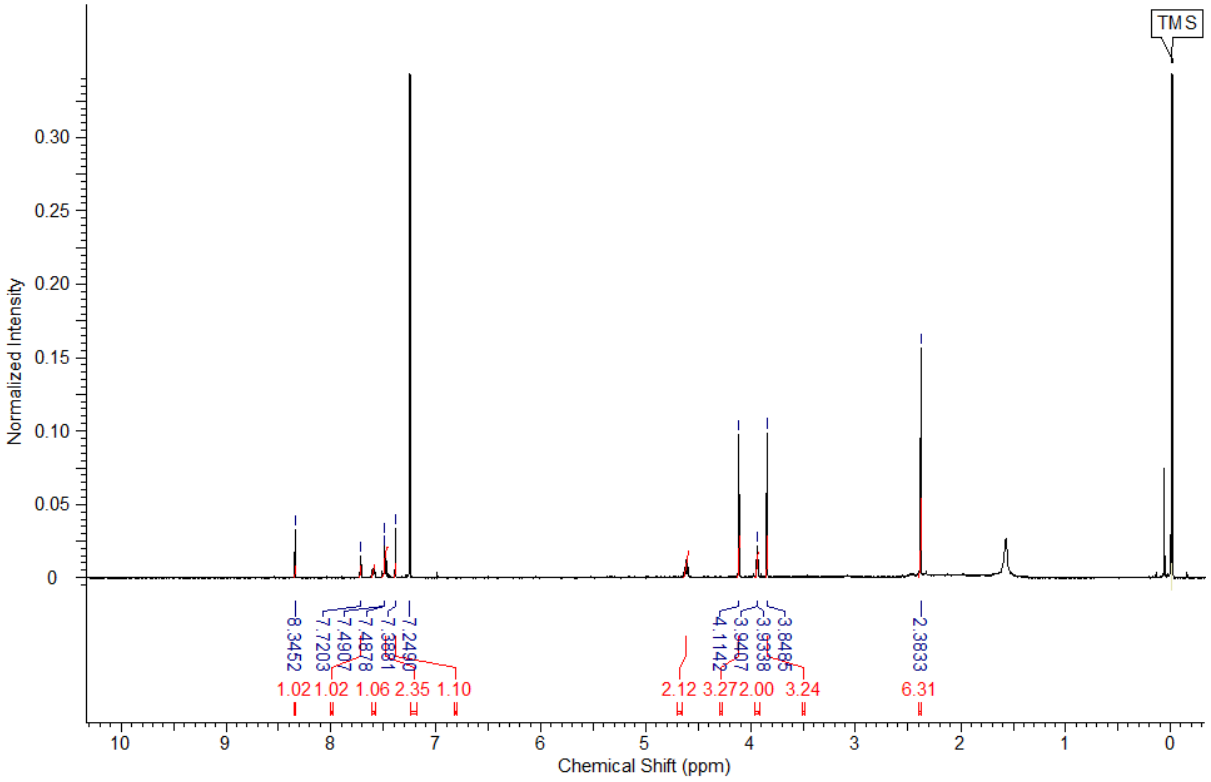

**1-(5-(4-chlorophenyl)-3-isobutyl-7,8-dimethoxy-3H-pyrazolo[3,4-c]isoquinolin-1-yl)-N,N-dimethylmethanamine (33)**

- Proton NMR of compound 33

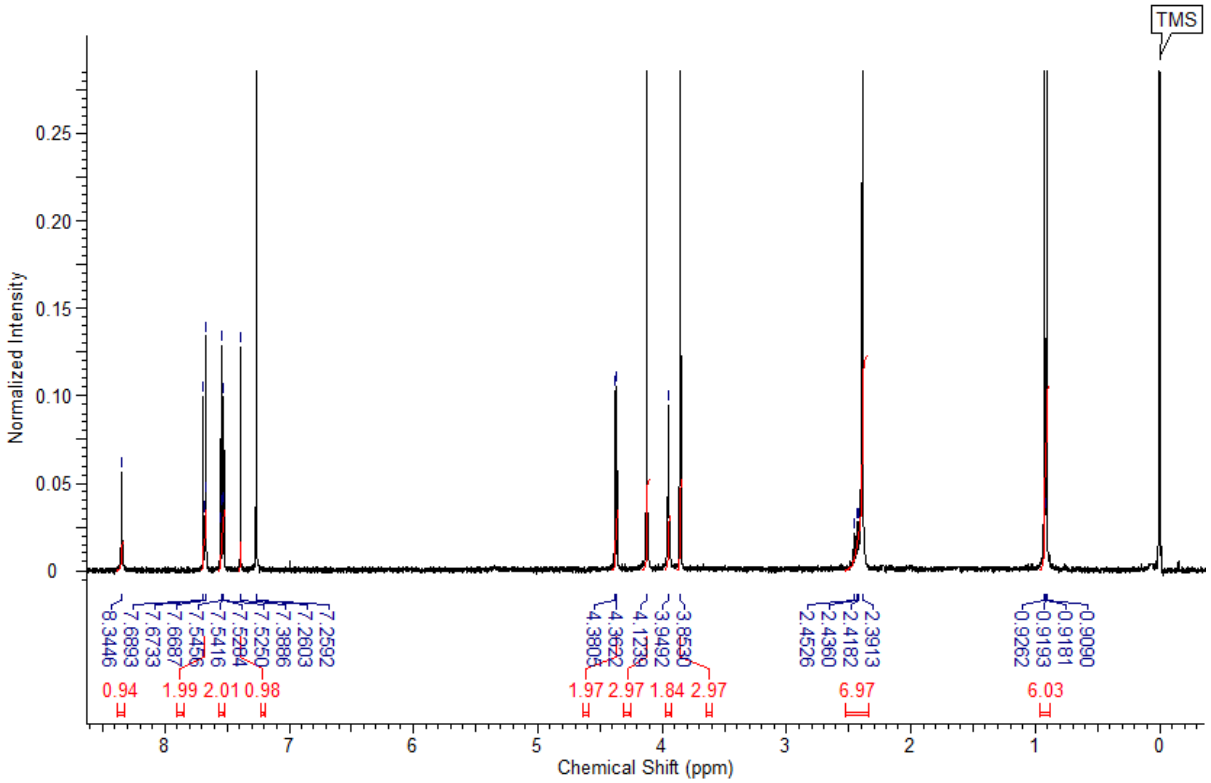


- Carbon NMR of compound 33

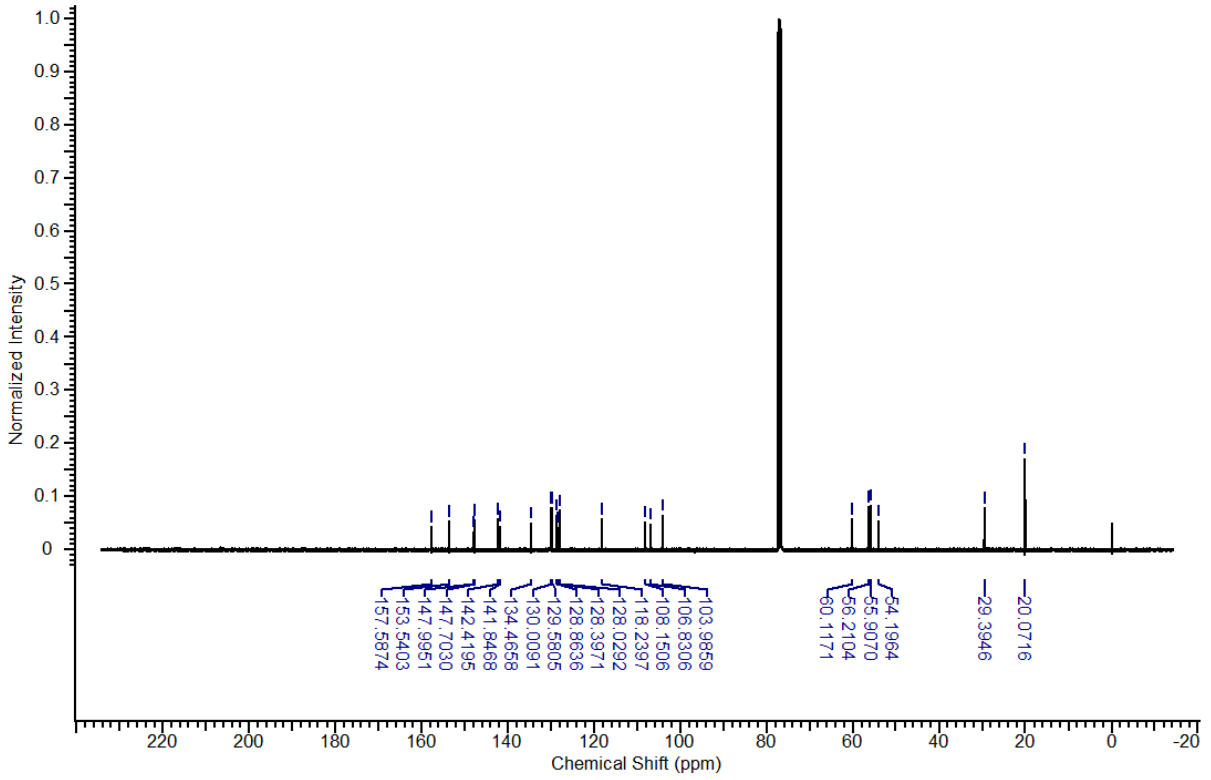

## 4. Spectroscopy of intermediate compounds

### 4-(3,4-dimethoxyphenyl)-3-(methoxymethyl)-1H-pyrazol-5-amine (6)

- Proton NMR of compound 6

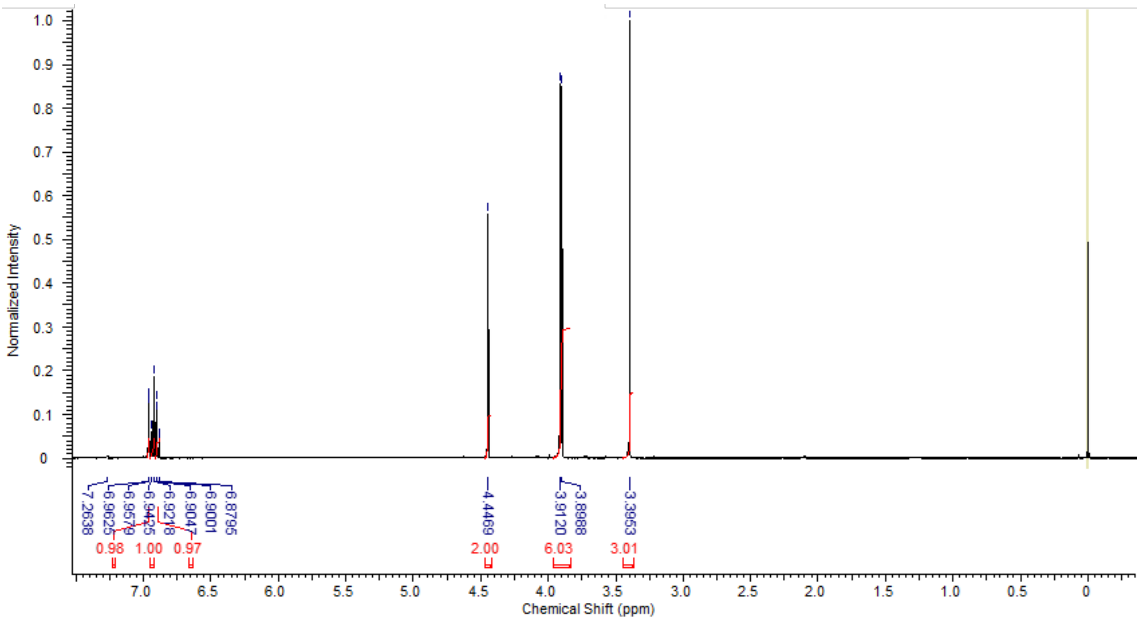


### 5-(3-chlorophenyl)-7,8-dimethoxy-1-(methoxymethyl)-3H-pyrazolo[3,4-c]isoquinoline (7a)

- Proton NMR of compound 7a

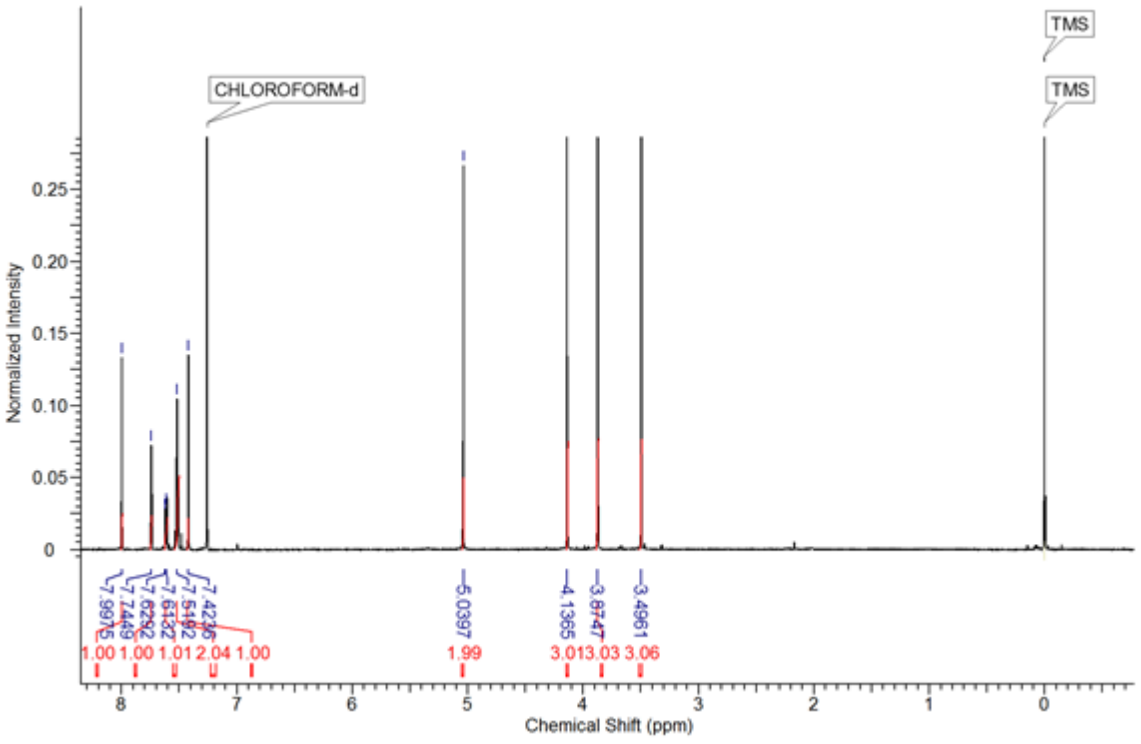

## 5-(4-chlorophenyl)-7,8-dimethoxy-1-(methoxymethyl)-3H-pyrazolo[3,4-c]isoquinoline (7b)

- Proton NMR of compound 7b

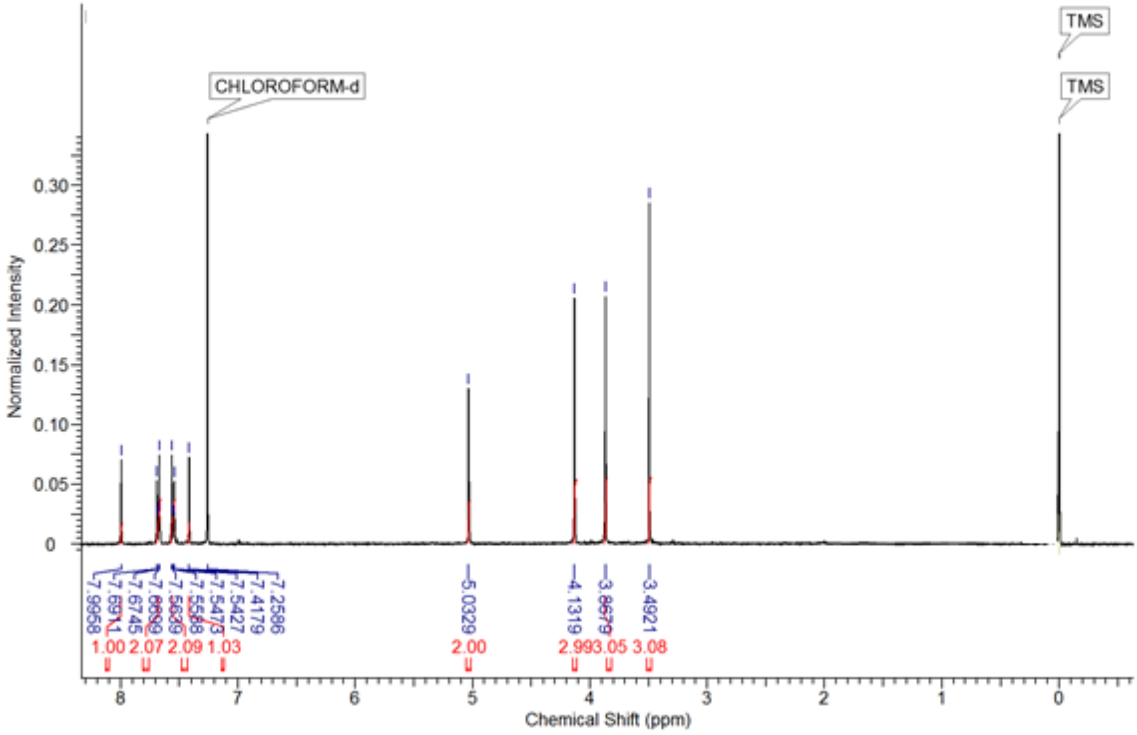


## 5-(2-chlorophenyl)-7,8-dimethoxy-1-(methoxymethyl)-3H-pyrazolo[3,4-c]isoquinoline (7c)

- Proton NMR of compound 7c

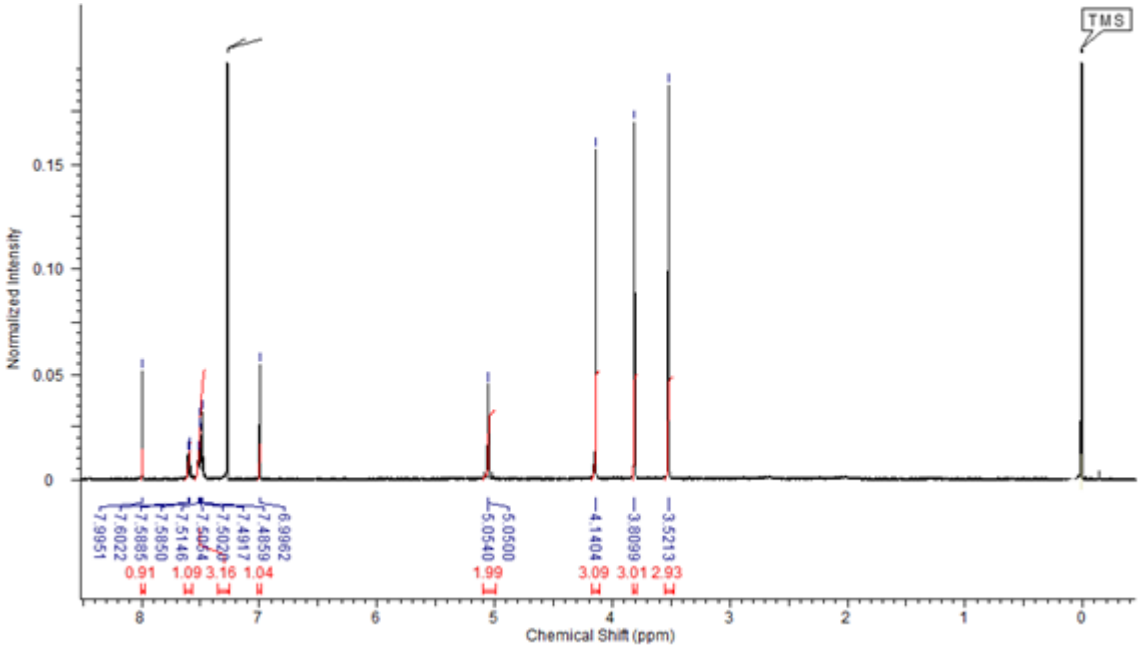

## (5-(3-chlorophenyl)-7,8-dimethoxy-3H-pyrazolo[3,4-c]isoquinolin-1-yl)methanol (8a)

- Proton NMR of compound 8a

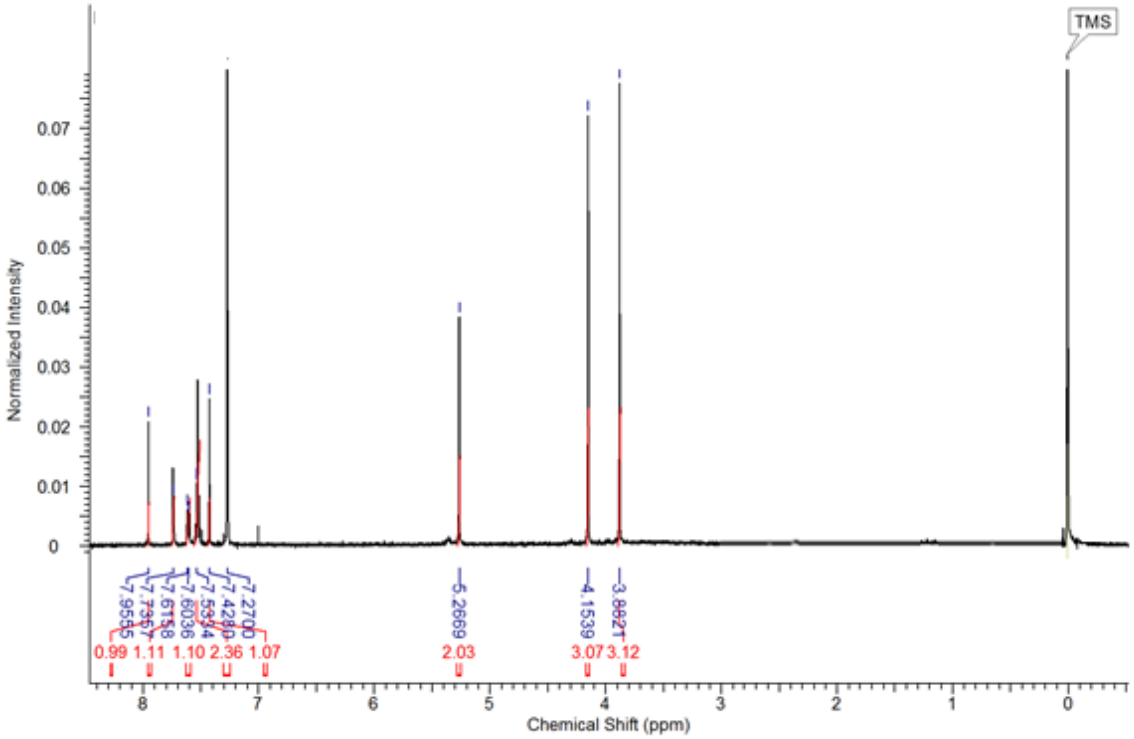


## (5-(4-chlorophenyl)-7,8-dimethoxy-3H-pyrazolo[3,4-c]isoquinolin-1-yl)methanol (8c)

- Proton NMR of compound 8b

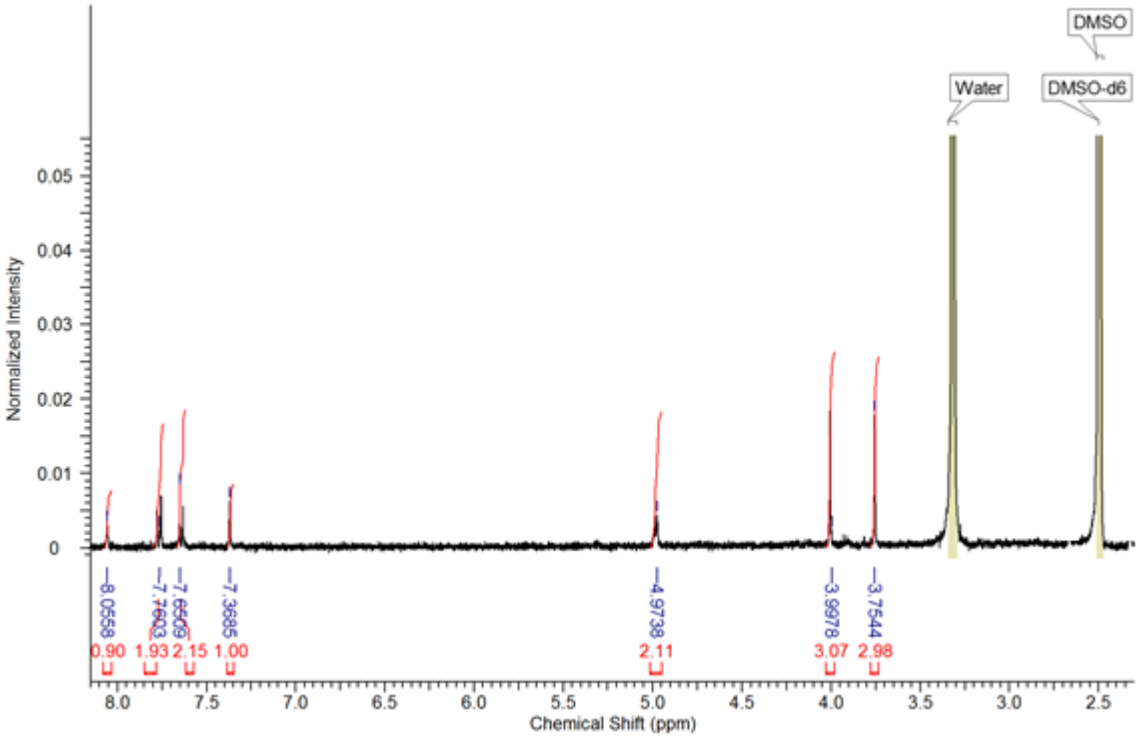

(5-(2-chlorophenyl)-7,8-dimethoxy-3H-pyrazolo[3,4-c]isoquinolin-1-yl)methanol (8c)

- Proton NMR of compound 8c

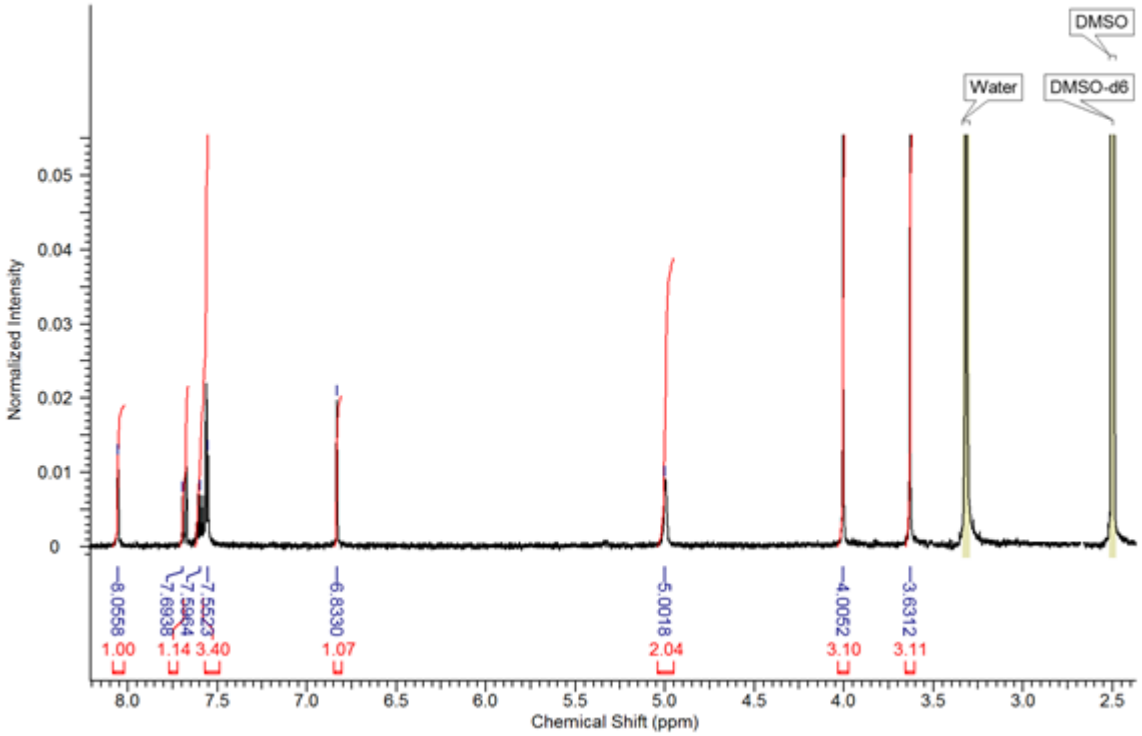


(5-(3-chlorophenyl)-7,8-dimethoxy-3H-pyrazolo[3,4-c]isoquinolin-1-yl)methanamine (9a)

- Proton NMR of compound 9a

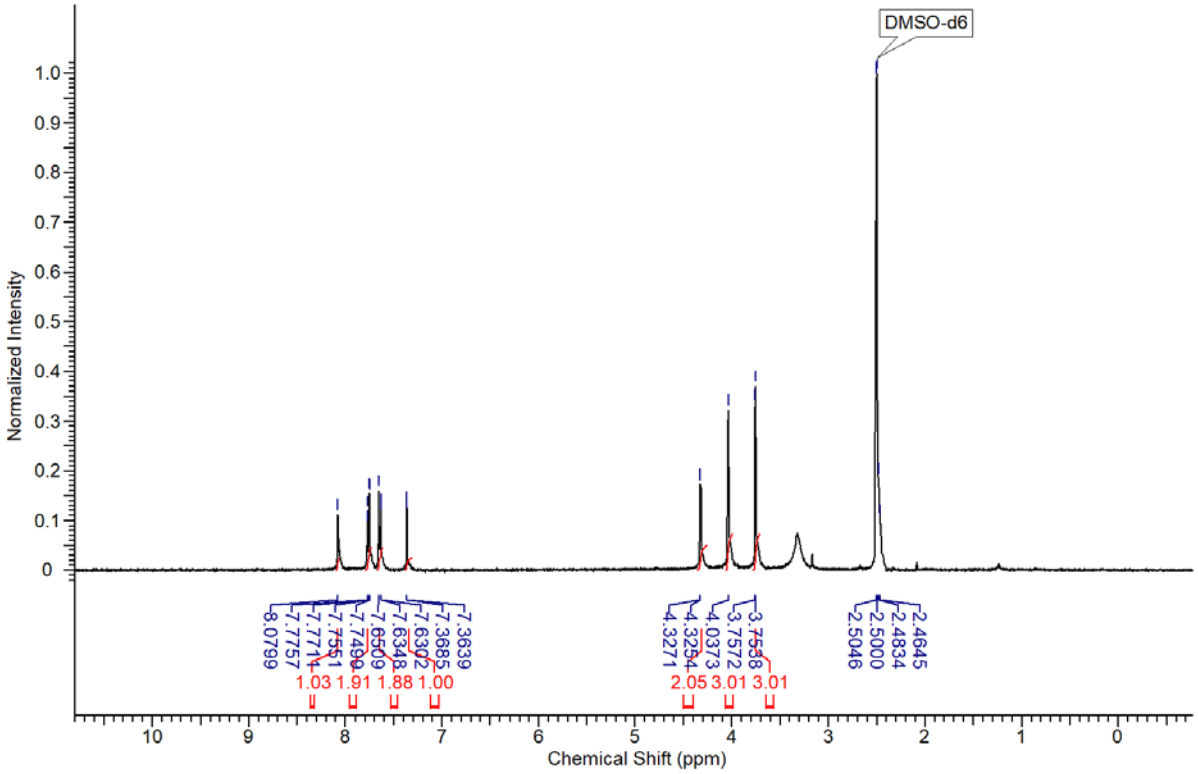

**(5-(4-chlorophenyl)-7,8-dimethoxy-3H-pyrazolo[3,4-c]isoquinolin-1-yl)methanamine (9b)**

- Proton NMR of compound 9b

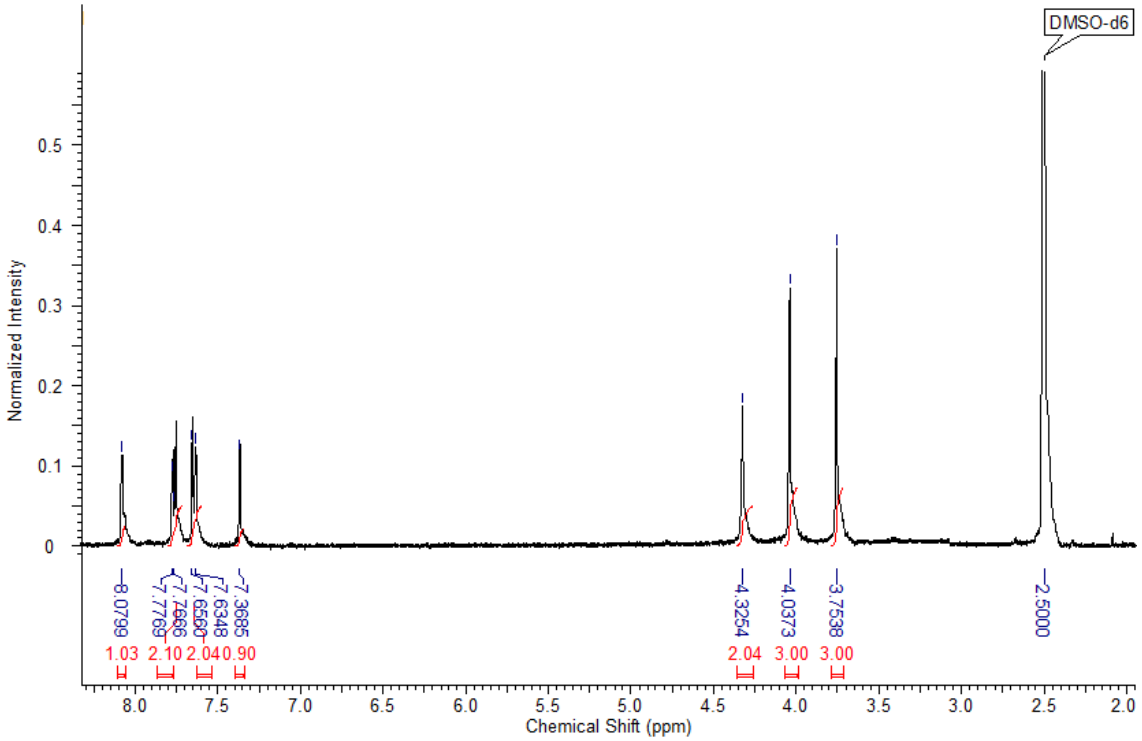


**(5-(2-chlorophenyl)-7,8-dimethoxy-3H-pyrazolo[3,4-c]isoquinolin-1-yl)methanamine (9c)**

- Proton NMR of compound 9c

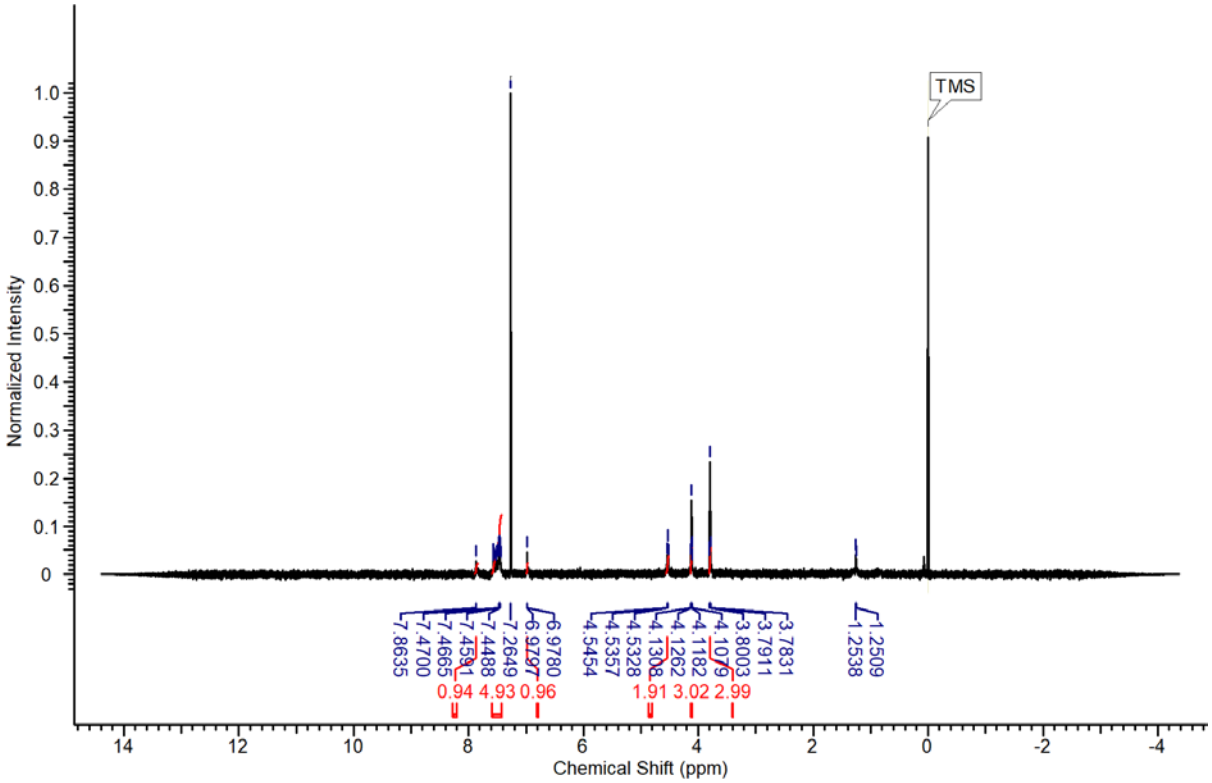

**tert-butyl ((5-(3-chlorophenyl)-7,8-dimethoxy-3H-pyrazolo[3,4-c]isoquinolin-1-yl)methyl)carbamate (10a)**

- Proton NMR of compound 10a

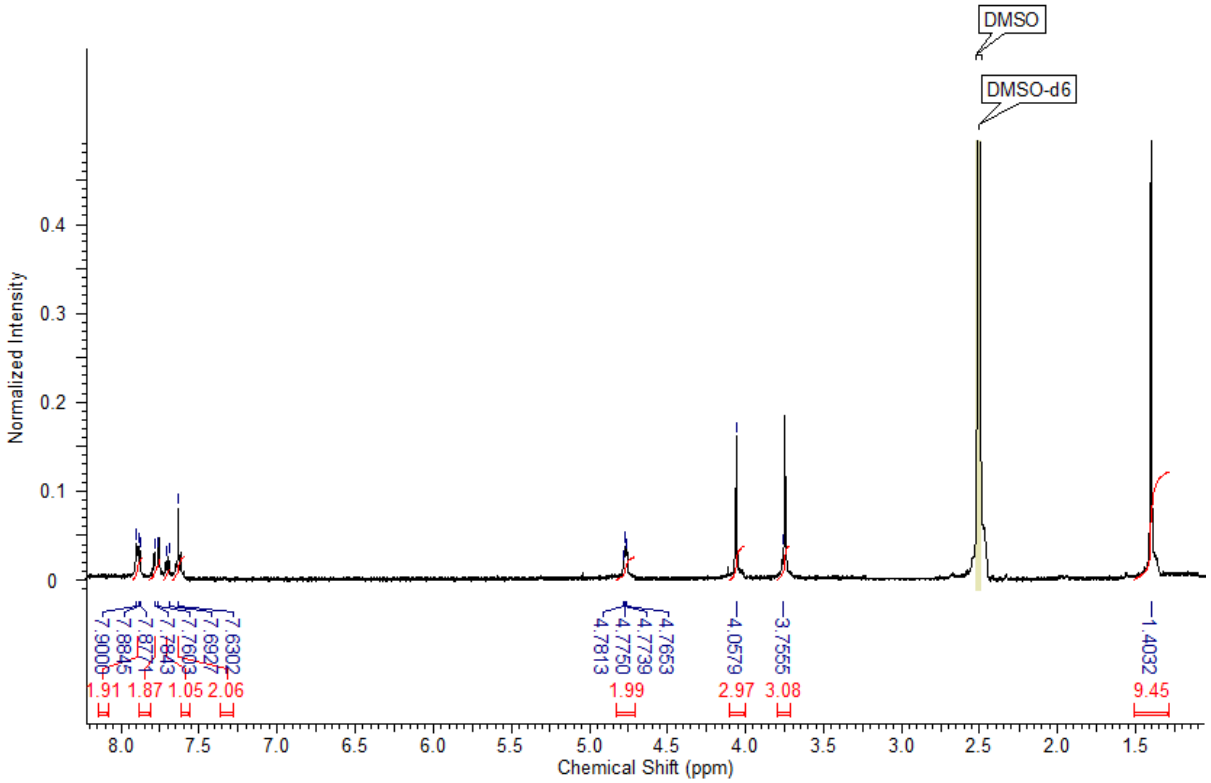


**tert-butyl ((5-(4-chlorophenyl)-7,8-dimethoxy-3H-pyrazolo[3,4-c]isoquinolin-1-yl)methyl)carbamate (10b)**

- Proton NMR of compound 10b

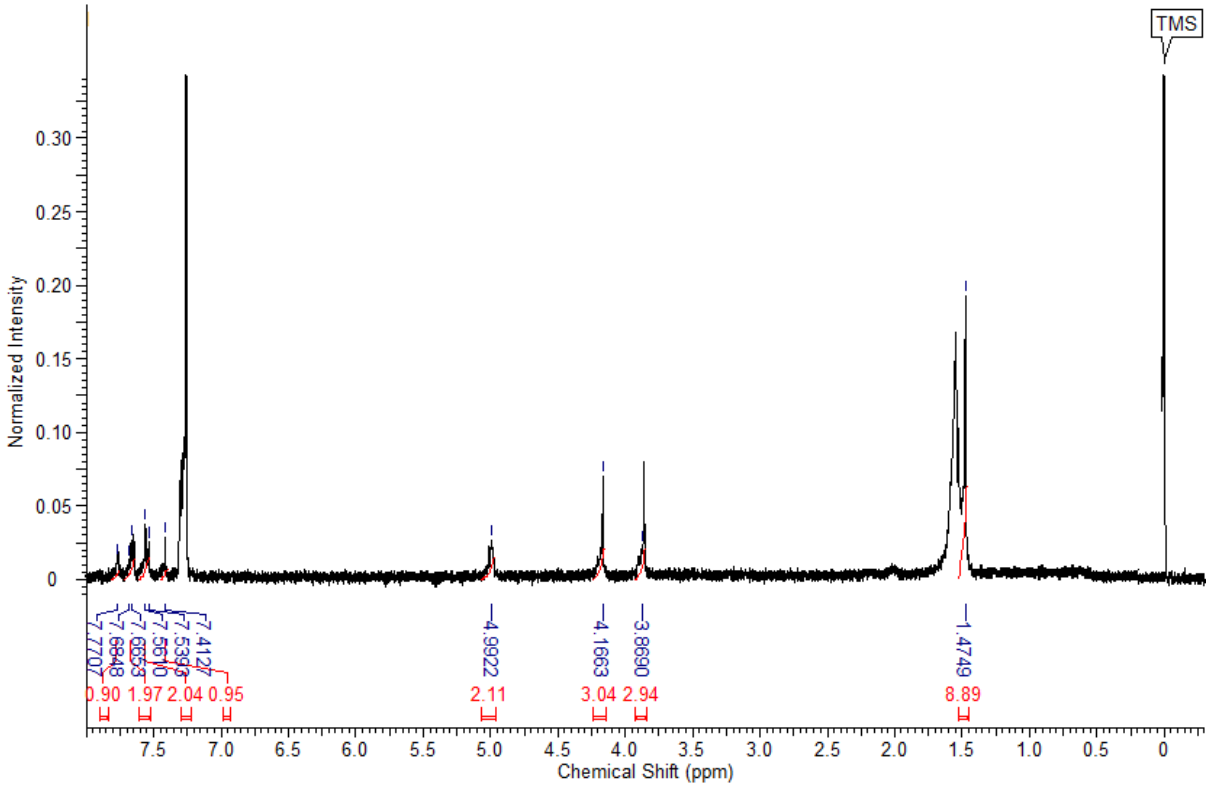

**tert-butyl ((5-(2-chlorophenyl)-7,8-dimethoxy-3H-pyrazolo[3,4-c]isoquinolin-1-yl)methyl)carbamate (10c)**

- Proton NMR of compound 10c

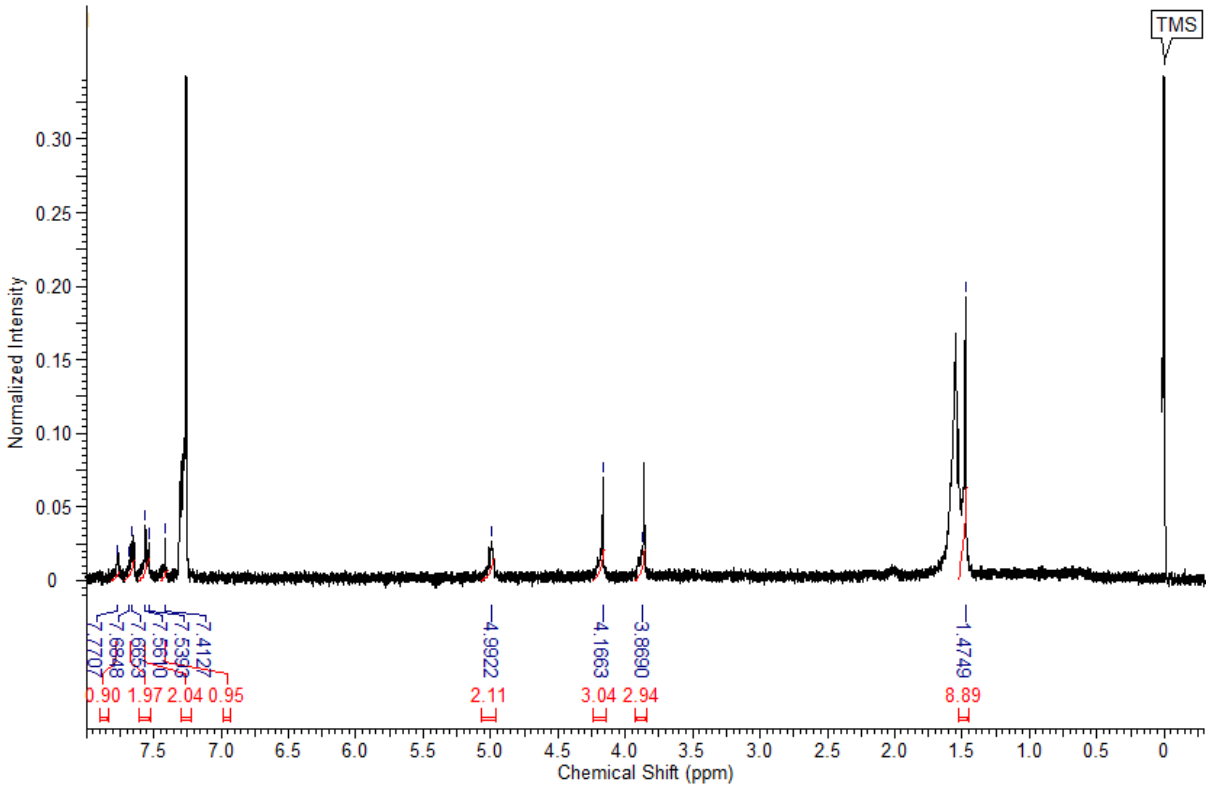


**tert-butyl ((5-(3-chlorophenyl)-7,8-dimethoxy-3-(naphthalen-2-ylmethyl)-3H-pyrazolo[3,4-c]isoquinolin-1-yl)methyl)carbamate (11d)**

- Proton NMR of compound 11d

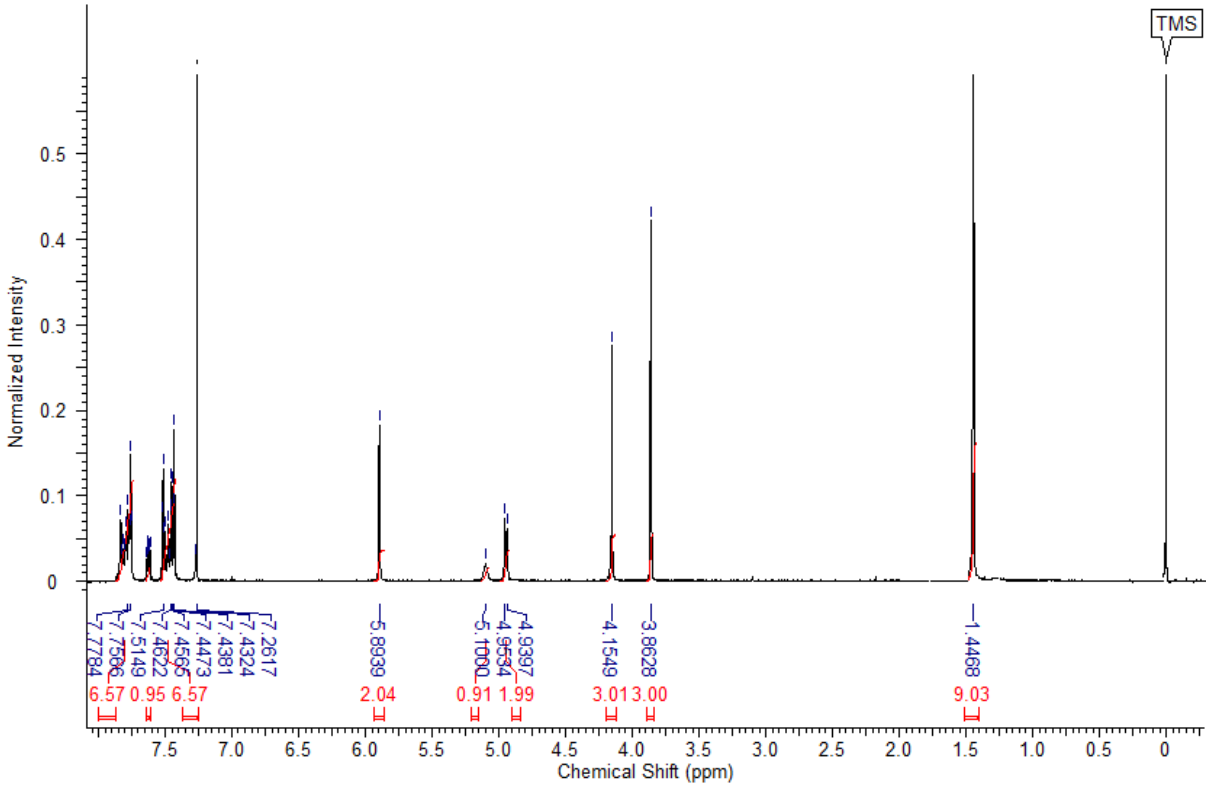

**Tert-butyl ((5-(4-chlorophenyl)-7,8-dimethoxy-3-(naphthalen-2-ylmethyl)-3H-pyrazolo[3,4-c]isoquinolin-1-yl)methyl)carbamate (11e)**

- Proton NMR of compound 11e

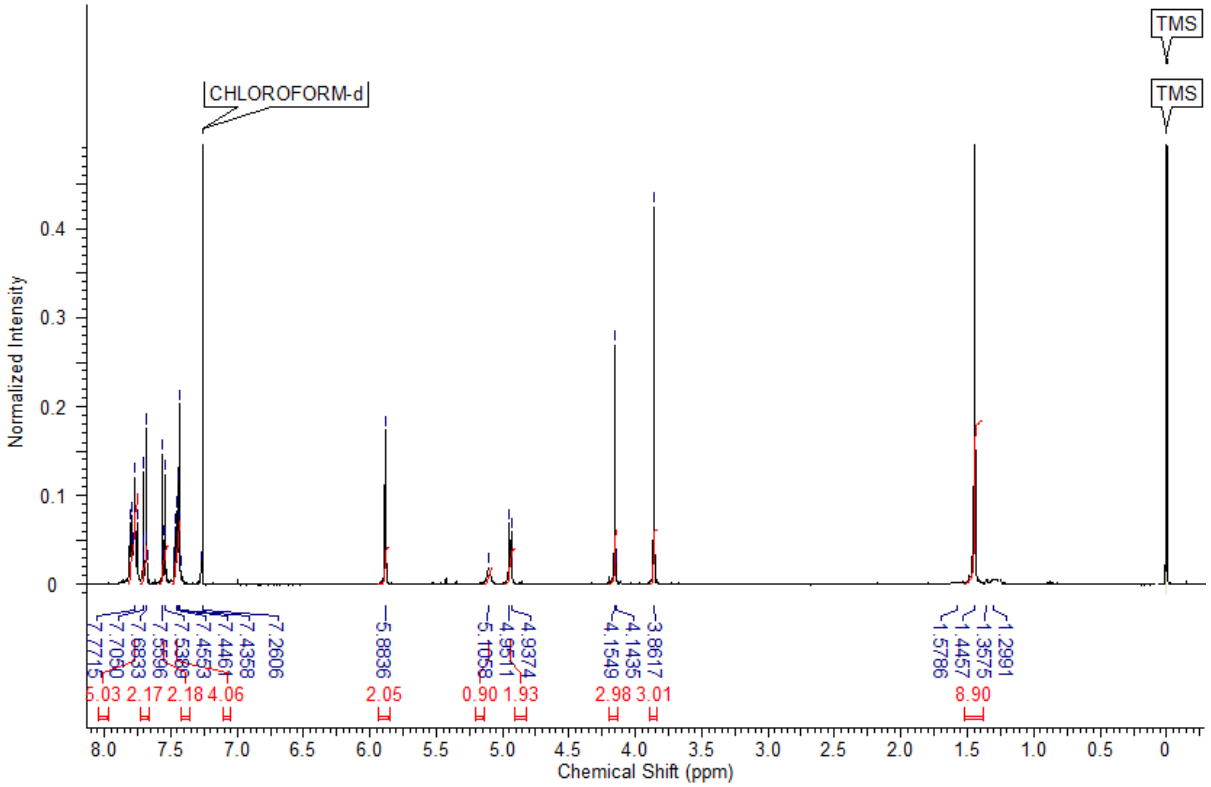


**1-(5-(3-chlorophenyl)-7,8-dimethoxy-3H-pyrazolo[3,4-c]isoquinolin-1-yl)-N,N-dimethylmethanamine (12a)**

- Proton NMR of compound 12a

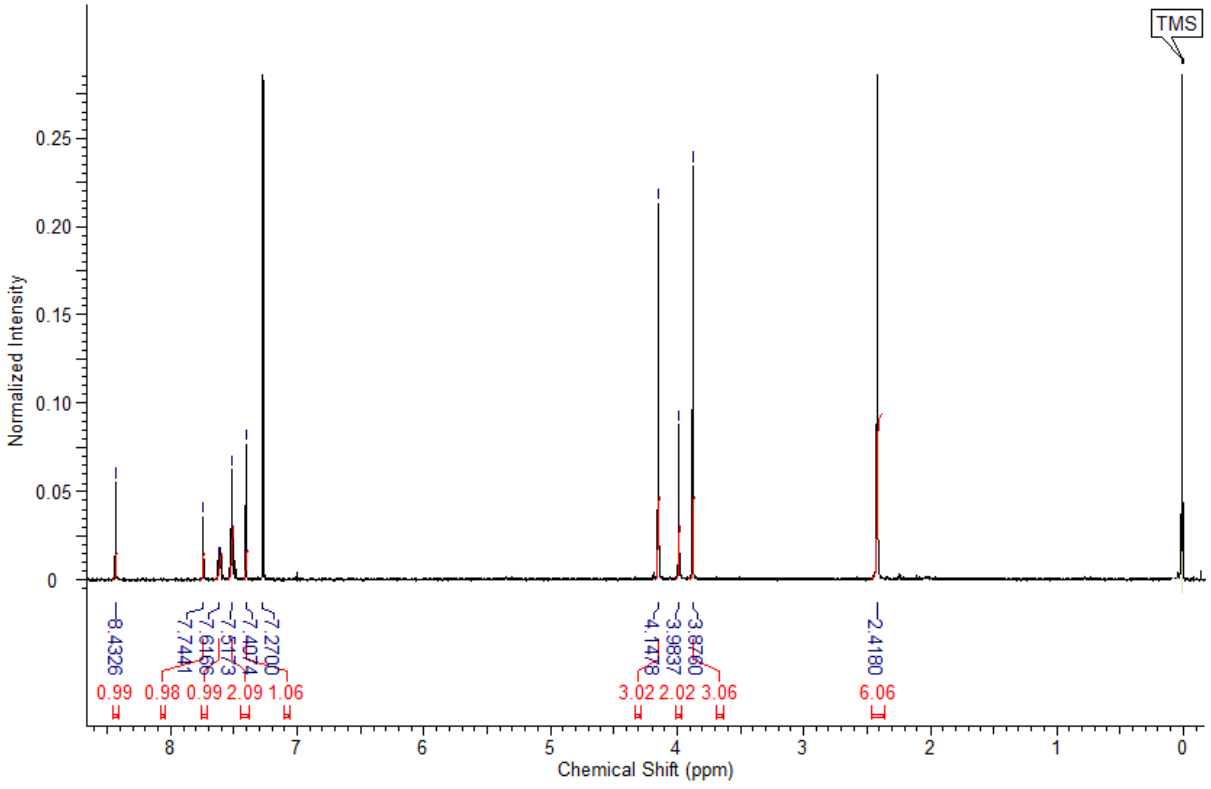

**1-(5-(4-chlorophenyl)-7,8-dimethoxy-3H-pyrazolo[3,4-c]isoquinolin-1-yl)-N,N-dimethylmethanamine (12b)**

- Proton NMR of compound 12b

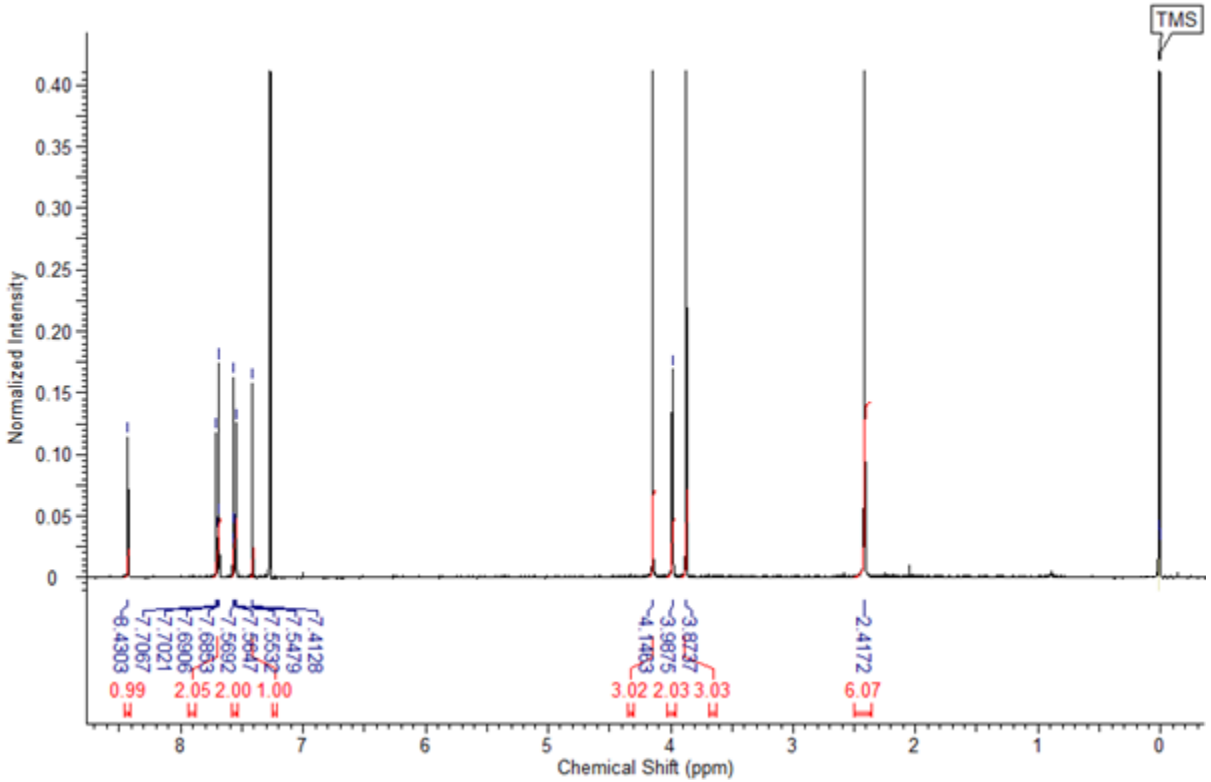


**1-(5-(2-chlorophenyl)-7,8-dimethoxy-3H-pyrazolo[3,4-c]isoquinolin-1-yl)-N,N-dimethylmethanamine (12c)**

- Proton NMR of compound 12c

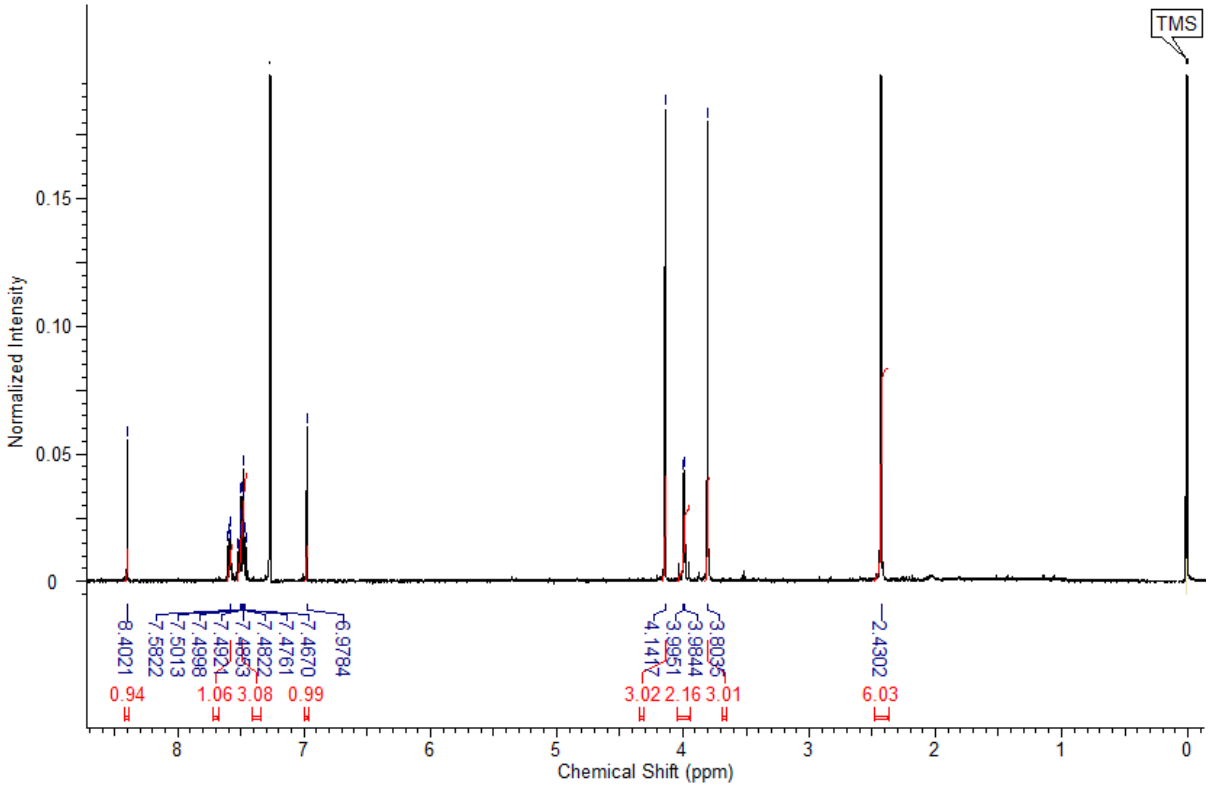

## 5. Selectivity of compound 15 and 19

### 5.1 % Activation of compound 15 and 19 against Human Kappa Opioid Receptor

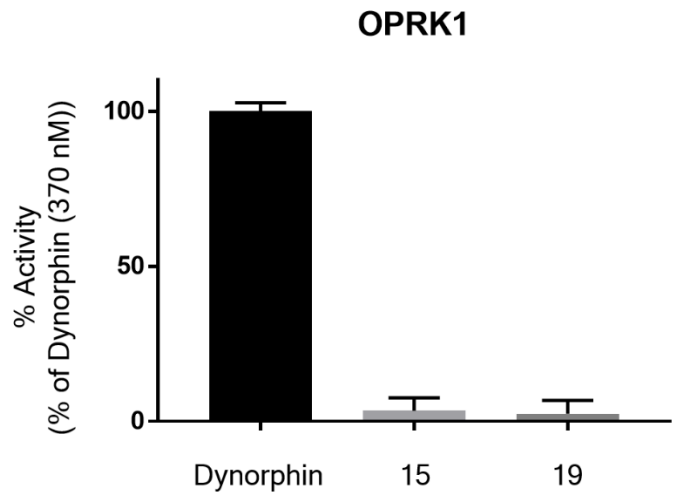


**Figure S4. % Activation of human κ-OR using FLIPR calcium efflux assay.** 10 μM of compound 15 and 19 were treated. Positive control Dynorphin (370 nM) was used to compare the data.

### 5.2 % Activation of compound 15 and 19 against Human Delta Opioid Receptor

We used Eurofins (Eurofins Scientific, Luxembourg) GPCR service to confirm the delta opioid agonism of compound 15 and 19.

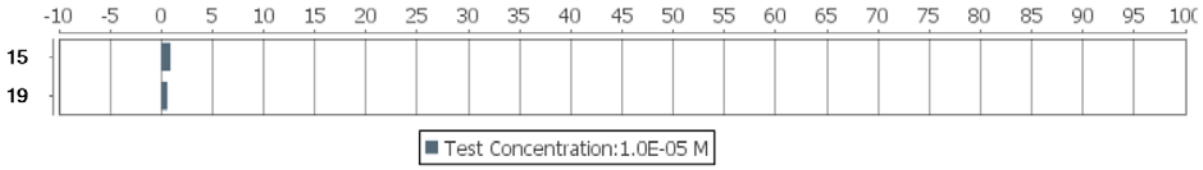


**Figure S5. % Activation of human δ-OR using fluorimetry calcium efflux assay.** 10 μM of compound 15 and 19 were treated. Positive control DPDPE (1 μM) was used to compare the data.

## 6. Synthesis of compound 4

Among the suggested 6 compounds, we were able to synthesize 4 successfully (Scheme S1). The commercially available 3,4-dimethoxy benzyl cyanide was reacted with ethyl methoxyacetate for the introduction of methoxy acetyl moiety at the benzyl position to afford compound **5**. Cyclization using hydrazine hydrate led to amino-methoxy-pyrazole compound **6**, which was subsequently reacted with aluminum trichloride under an argon atmosphere to yield mixtures of compound **34** and its isomer product, 5-(5-amino-3-((dibenzylamino)methyl)-1H-pyrazol-4-yl)-2-methoxyphenol. The cyclization of this mixture under microwave conditions with 4-chlorobenzaldehyde afforded compound **35**. In this step, only compound **34** was cyclized because of the position of the methoxy electron donating group. After selective O-demethylation using boron tribromide (**36**), the benzyl alcohol moieties were transformed to corresponding chlorides followed by primary amines through reactions using thionyl chloride and 2M ammonia solution in THF, respectively to provide compound **37**. Compound **38** was prepared by protection of the amine with di-*tert*-butyl-dicarbonate. The phenolic moiety was protected with THP group (**39**) and then, N-alkylation of pyrazole moiety provided compound (**40**). The final product compound **4** was obtained by deprotection of the Boc & THP groups in strong acidic condition using trifluoroacetic acid.

**Scheme S1. Synthesis of compound 4**. (a) potassium tert-butoxide, THF, RT, 2 h, 55%; (b) Hydrazine hydrate, AcOH, MeOH, reflux, 4 h, 60%; (c) $AlCl_3$, DCM, 2 h, 67%; (d) 4-chloro benzaldehyde, TFA, Microwave irradiation, 140°C, 2 h, 44%; (e) BBr3, DCM, 0°C, 4 h, 45%; (f) thionyl chloride, reflux, 2 h, *then* 2M ammonia solution in THF solution, THF 65%; (g) di-tert-butyl dicarbonate, TEA, DCM, RT, 1 h 71%; (h) 3,4-dihydro-2H-pyran, MsOH, DCM, RT, 1 h, 85%; (i) Halides, NaH, DMF, RT, 72%; (j) TFA, DCM, 0°C, 2 h, then TFA, MeOH, 0°C 62%.

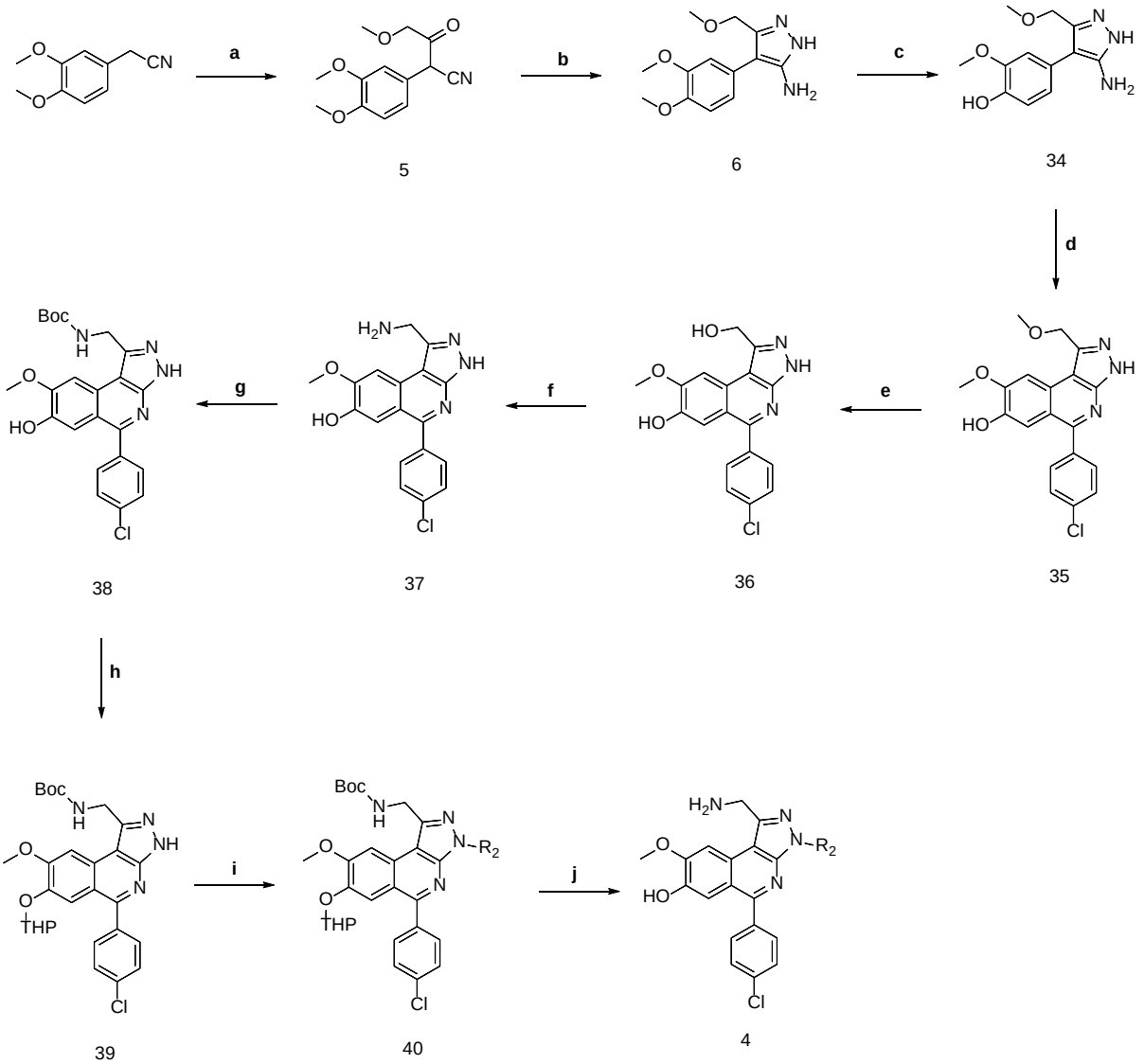

**1-(aminomethyl)-5-(4-chlorophenyl)-3-(4-hydroxybenzyl)-8-methoxy-3H-pyrazolo[3,4-c]isoquinolin-7-ol (4)**

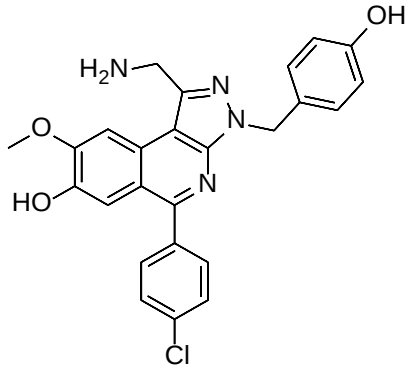


A solution of compound **40** (15 mg, 0.023 mmols) in dichloromethane (2 ml) and methanol (2 ml) were cooled to 0°C, and trifluoro acetic acid (2 ml) was slowly added. Upon completion of reaction, the mixture was concentrated under reduced pressure. The residue was purified by silica gel column chromatography with MeOH: ammonia saturated $CHCl_3$ (5%) to afford **4** as a yellow liquid.

$^1$H NMR (400 MHz, DMSO-*d*6) δ 9.03 (s, 1 H), 7.66 – 7.33 (m, 2 H) ,7.55 – 7.62 (m, 2 H), 7.31 (s, 1 H), 6.75 (d, *J*=8.24 Hz, 2 H), 6.55 (d, *J*=8.24 Hz, 2 H), 4.65 (s, 2 H), 3.91 (s, 2 H), 3.72 (s, 3 H).

## References


[1] aS. K. Kim, L. Riley, R. Abrol, K. A. Jacobson, W. A. Goddard, 3rd, *Proteins* **2011**, *79*, 1878-1897; bC. E. Scott, R. Abrol, K. H. Ahn, D. A. Kendall, W. A. Goddard, 3rd, *Protein science : a publication of the Protein Society* **2013**, *22*, 101-113; cR. Berro, A. Yasmeen, R. Abrol, B. Trzaskowski, S. Abi-Habib, A. Grunbeck, D. Lascano, W. A. Goddard, 3rd, P. J. Klasse, T. P. Sakmar, J. P. Moore, *Journal of virology* **2013**, *87*, 6569-6581; dA. Kirkpatrick, J. Heo, R. Abrol, W. A. Goddard, 3rd, *Proceedings of the National Academy of Sciences of the United States of America* **2012**, *109*, 19988-19993; eL. Charlier, J. Topin, C. Ronin, S. K. Kim, W. A. Goddard, 3rd, R. Efremov, J. Golebiowski, *Cellular and molecular life sciences : CMLS* **2012**, *69*, 4205-4213; fJ. Tan, R. Abrol, B. Trzaskowski, W. A. Goddard, 3rd, *Journal of chemical information and modeling* **2012**, *52*, 1875-1885.

[2] aR. Abrol, A. R. Griffith, J. K. Bray, W. A. Goddard, 3rd, *Methods in molecular biology* **2012**, *914*, 237-254; bR. Abrol, S. K. Kim, J. K. Bray, B. Trzaskowski, W. A. Goddard, 3rd, *Methods in enzymology* **2013**, *520*, 31-48; cR. Abrol, J. K. Bray, W. A. Goddard, 3rd, *Proteins* **2011**; dJ. K. Bray, R. Abrol, W. A. Goddard, 3rd, B. Trzaskowski, C. E. Scott, *Proceedings of the National Academy of Sciences of the United States of America* **2014**, *111*, E72-78.

[3] W. M. Huang, A.; Venkatakrishnan, A.J.; Laeremans, T.; Feinberg, E.N.; Sanborn, A.L.; Kato, H.E.; Livingston, K.E.; Thorsen, T.S.; Kling, R.C.; Granier, S.; Gmeiner, P.; Husbands, S.M.; Traynor, J.R.; Weis, W.I.; Steyaert, J.; Dror, R.O.; Kobilka, B.K., *Nature* **2015**, *524*, 315-321.

[4] A. Manglik, Kruse, A.C., Kobilka, T.S., Thian, F.S., Mathiesen, J.M., Sunahara, R.K., Pardo, L., Weis, W.I., Kobilka, B.K., Granier, S., *Nature* **2012**, *485*, 321- 323.

[5] G. G. Fenalti, P.M.; Katritch, V.; Huang, X.P.; Thompson, A.A.; Cherezov, V.; Roth, B.L.; Stevens, R.C., *Nature* **2014**, *506*, 191-196.

[6] A. A. L. Thompson, W.; Chun, E.; Katritch, V.; Wu, H.; Vardy, E.; Huang, X.P.; Trapella, C.; Guerrini, R.; Calo, G.; Roth, B.L.; Cherezov, V.; Stevens, R.C., *Nature* **2012**, *485*, 395-399.